

## Reviewer 1:

Comments: The manuscript named “Investigation of CATS aerosol products and application toward global diurnal variation of aerosols” by Lee et al. presents an inter-comparison of the measurements of aerosol optical depth and mean profiles between CATS and other remote sensing sensors (AERONET, MODIS, and CALIOP) for a period of Feb. 2015 -Oct. 2017. This paper also discusses the aerosol diurnal variation patterns changing with different seasons and geographic regions. This manuscript presents an original data analysis of some significant instruments. The discussion and conclusions are sound and clear. Therefore, I recommend for publish after addressing some minor concerns.

*Response: We thank the reviewer for his/her suggestions, comments and encouragement.*

Comments: Specific comments: Section 2, can you briefly describe the AOD measurement uncertainty of these instrument?

*Response: This is a great question. Most validation and uncertainties analysis efforts of satellite AOD retrievals are focus on visible channels. To our knowledge, uncertainties in AOD retrieval at 1064 nm, both from passive and active sensors, are less studied. Just as suggested from the comments from Mark Vaughan and Stuart Young (Short comment for this paper), this paper might be among the first to go deep into AOD retrievals at 1064 nm channel. We were not able to find papers to address uncertainties in AOD retrievals at 1064 nm, although there are papers that do show comparisons between CALIOP and AERONET AOD at 1064 nm (Omar et al., 2013).*

*Omar, A. H., D. M. Winker, J. L. Tackett, D. M. Giles, J. Kar, Z. Liu, M. A. Vaughan, K. A. Powell, and C. R. Trepte (2013), CALIOP and AERONET aerosol optical depth comparisons: One size fits none, J. Geophys. Res. Atmos., 118, 4748–4766, doi:10.1002/jgrd.50330.*

*We have added the following discussion in the text: “Note that most evaluation efforts for passive- and active-based AOD retrievals are focused on the visible spectrum and the performance of AOD retrievals at the 1064 nm channel is less explored. “*

Comments: P6, L134, it may be better to replace “increasing” with “degrading”.

*Response: Done*

Comments: P8, L163, can you describe what constant value of that Angstrom exponent is used here without letting readers to look for that in Shi et al. paper?

*Response: We apologize for the confusion. The Angstrom exponent values are computed using instantaneous retrievals. We have revised the text to avoid confusion.*

*“Here we assume the angstrom exponent value, computed using instantaneous AOD retrievals at the 860 and 1240 nm, remains the same for the 860 to 1064 nm wavelength range, similar to what has been suggested by Shi et al., (2011; 2013). “*

Comments: P12,L266-268, “A clear diurnal variation is found, with the peak mean AOD of 0.08 found around local noon and smaller AOD values of 0.06 found for both sunrise and sunset times.” In Figure 4, look to me the AOD peak is located around 9AM local time, “before” the noon. Also, is this diurnal variation consistent with your expectation?

*Response: Thanks for the suggestion. We have revise the sentence to “with the mean AOD values of 0.07-0.08 found between late morning and early afternoon and smaller AOD values of 0.06 found for both sunrise and sunset times”*

Comments: Can you provide an explanation on why the AOD measured by CATS less than all other instruments suggested by Figure 1, 2, and 3?

*Response: We assume that the reviewer is referring to the slope of the regressions in Figures 1-3. Slopes in linear regressions can often be biased by outliers. In Figure 6, which are spatial plots of AODs from CALIOP and CATS, differences are less noticeable for the DJFMAM season. For the JJASON season, CATS AODs are lower at certain regions (Middle East, India, and North Africa) and higher over other regions (South Africa). The cause of those discrepancies, however, is unclear to us. To really explore the issue, it deserves a paper of its own. Thus, we leave this topic to a future paper.*

## **Reviewer 2:**

Comments: The authors use more than two years of CATS data to examine the diurnal cycles of the aerosol loading on global scale. Their results show that a strong peak at 6 am local time in aerosol extinction profile over North Africa during the June-November season. This finding is exciting and brand new. I would recommend this manuscript be published in ACP after a few minor changes

*Response: We thank the reviewer for his/her encouragement and his/her thoughtful comments*

Comments: (1) In Figure 5, there are some spikes above 2 km in the aerosol extinction vertical profiles seen in the CATS data, but not present in the CALOP data. Are they due to the cloud screening differences between CATS and CALIOP?

*Response: We suspect that the high spikes were introduced by a bug in the code which allowed a very small number of larger extinction values through. This has been fixed, and the spikes are no longer present. The overall shapes of the profiles remain unchanged.*

Comments: (2) Line# 353-354, unlike CALIOP, MODIS Aqua aerosol products are only available in the early afternoon, but not in the early morning, since the algorithm only performs retrieval over daytime.

*Response: We have revised the sentence to “as CALIOP provides early morning and afternoon over passes, and Aqua MODIS has an over pass time after local noon, ”*

Comments: (3) Line# 355-356, please add a sentence or two to briefly elaborate what aerosol above cloud issues are as reported by Rajapashe et al., (2017).

*Response: This study has been explained in Section 2.2. To avoid duplication, we have revised the sentence to “It is also possibly due to aerosol above cloud related issues as reported by Rajapakshe et al. (2017), as explained in Section 2.2”*

Comments: (4) Line# 358, please spell out “AGL”.

*Response: Done. We have added “Above Ground Level (AGL)”*

Comments: (5) The aerosol extinction at 1064 nm may not be as sensitive to the fine mode aerosols (such as smoke and urban pollutant aerosols) compared to the coarse mode aerosols (such as dust). The authors probably should add a few sentences to address this

*Response: Great point. We have added the following discussions to address this issue. "Still, readers shall be aware that AOD retrievals at the 1064 nm are less sensitive to fine mode aerosols such as smoke and pollutant aerosols, compared to coarse mode aerosols such as dust aerosols. Thus, an investigation of diurnal variations of aerosol properties at the visible channel may be also needed for a future study."*

## Short Comments by Mark Vaughan and Stuart Young

Comments: This paper compares the aerosol extinction profiles and aerosol optical depths (AODs) retrieved by the CATS lidar with similar quantities retrieved by AERONET, MODIS, and CALIOP. To our knowledge, this is the first ever in-depth assessment of satellite-derived AODs measured/retrieved in the near-infrared, and thus should be of great interest to several different groups in the aerosol research community. Overall, the authors have done a good job in bringing multiple analyses together. However, we find several places where additional analyses are warranted and where more in-depth discussions will help strengthen the final manuscript.

*Response: We thank Mark Vaughan and Stuart Young and we appreciate the suggestions and comments which we believe are shaping this paper into a better paper*

## General Remarks

Comments: When filtering the extinction coefficients retrieved from the CATS and CALIOP measurements, the authors say that candidate extinction coefficients were constrained to a “nominal range” of 0 to  $1.25 \text{ km}^{-1}$ , and that “all near zero negative values” are set to zero (page 6, lines 114–119). Presumably these “near zero negative values” that were set to zero were not actually removed from consideration, but instead were included in subsequent data averaging operations (the writing in this section is not sufficiently clear on this point). Changing negative values to zeros prior to averaging is not statistically valid, as it guarantees high biases in the estimated mean values. Reporting these high biases erroneously improves the comparisons of lidar-derived optical depths with those obtained by other sensors. To avoid this, all CATS and CALIOP mean values should be correctly recalculated before the final version of this manuscript is published.

*Response: This is an excellent point. First, when calculating AOD and AOD climatology, we used the CATS and CALIOP derived AOD values. Thus, this is no need for us to detailing with negative extinction coefficients and we have revised the paper to reflect the issue. We did, however, apply the constraint that AOD values which came from retrievals containing extinction coefficients greater than  $1.25 \text{ km}^{-1}$  be excluded to avoid using AOD values from what are likely cloud contaminated profiles. We have added the following discussions.*

*“In AOD related studies, CAT and CALIOP reported AOD values are used. However, although not derived in this study, only AOD values with corresponding aerosol vertical extinction that meet the QA criteria as mentioned in Sections 2.1 and 2.2 were used.”*

*Still, the extinction coefficients are used in estimating aerosol vertical distributions. As suggested we have revised our calculations and included those negative values, instead of setting them to zero. Note that similar approaches have been adopted for passive-based AOD studies, where*

negative AODs are used to reduce high bias in long term studies (Remer et al., 2005). We have made the changes in the text accordingly.

“Extinction was also constrained using a threshold as provided in the CATS data catalog ( $Extinction\_Coefficient_{1064\_Fore\_FOV} \leq 1.25 \text{ km}^{-1}$ ), similar to several previous studies (Redemann et al., 2012; Toth et al., 2016). Only profiles with extinction coefficient values less than  $1.25 \text{ km}^{-1}$  are included in this study. Small negative extinction coefficient values, however, are included in aerosol profile related analysis, to reduce potential high biases in computed mean profiles. Note that a similar approach has also been conducted in deriving passive-based AOD climatology (e.g. Remer et al., 2005).”

Remer, L.A., Y.J. Kaufman, D. Tanré, S. Mattoo, D.A. Chu, J.V. Martins, R. Li, C. Ichoku, R.C. Levy, R.G. Kleidman, T.F. Eck, E. Vermote, and B.N. Holben, 2005: [The MODIS Aerosol Algorithm, Products, and Validation](https://doi.org/10.1175/JAS3385.1). *J. Atmos. Sci.*, **62**, 947–973, <https://doi.org/10.1175/JAS3385.1>

Comment: While the main body of the text emphasizes the correlations between the CATS retrievals and the other data sets (e.g., lines 186–208), the authors do not provide any quantitative statements about the magnitudes of the CATS AODs or the differences between the different AOD estimates. Given that this paper is (to our knowledge) the first ever in-depth look at 1064 nm AOD, tables showing global and regional mean values and quantifying the CATS AOD estimates relative to the other sensors would add significantly to the value delivered by this paper. Profiles of the relative CATS-CALIOP extinction coefficient differences (i.e.,  $(CATS(z) - CALIOP(z)) / CALIOP(z)$ ) would be especially interesting.

Response: We have added a table to include regional and global means. Still, we documented that the differences may also be introduced by sampling differences of the sensors.

“Table 2. CALIOP and CATS mean aerosol optical depth for regions as highlighted in Figure 6 and globally between  $\pm 52^\circ$  latitude.”

Region	Latitude	Longitude	Mean CATS AOD (DJFMAM/JJASON)	Mean CALIOP AOD (DJFMAM/JJASON)
Global	52°S-52°N	180°W-180°E	0.09/0.10	0.09/0.09
India	7.5°N - 32.5°N	65°E - 85°E	0.22/0.26	0.22 /0.28
Africa - North	2.5°N - 22.5°N	35°W - 20°E	0.26/0.23	0.30 /0.25
Africa - South	17.5°S - 2.5°N	0° - 30°E	0.14/0.22	0.15 /0.13
Middle East	12.5°N - 27.5°N	35°E - 50°E	0.22/0.33	0.26/0.35
China	27.5°N - 37.5°N	110°E - 120°E	0.19/0.18	0.21 /0.16

*We have also added a plot of the difference (CATS(z)-CALIOP(z)) in Appendix A. As CALIOP extinction values become very small, the ratio of (CATS(z)-CALIOP(z))/CALIOP(z) has a tendency to grow very large from just a few data points and greatly impacts the standard deviation. Thus we plotted only the difference and did not include (CATS(z)-CALIOP(z))/CALIOP(z) and error bars with this particular plot.*

Comment: In section 3.1.1., CATS observations are compared with other observations made within  $\pm 30$  mins and  $\pm 0.4$  degrees. For aerosols, this is probably not too much of a problem a lot of the time, but we have seen numerous cases where there can be large differences in the scenes being observed (e.g., see Omar et al., 2013: “In 45% of the coincident instances CALIOP and AERONET do not agree on the cloudiness of the scenes.”). For AERONET, the comparisons may be improved by imposing another criterion, i.e., that the AERONET AODs made at the closest times preceding and following the CATS observations not vary by more than x%. A similar filter for potential spatial differences could include wind speed and direction (e.g., Lopes et al., 2013) and the spatial separations of the AERONET sites and the CATS observations. (This is likely to be quite a bit messier.)

*Response: We have included the references as suggested and reminded readers that the collocation criteria may have impacts to the results due to the spatial and temporal sampling methods chosen.*

*“Note that as suggested by Omar et al., 2013, the choices of spatial and temporal collocation windows have an effect on collocation results. However, we consider this as a topic beyond the scope of this study”*

Comment: While the authors point out a number of differences between the CATS retrievals and those derived from other sensors, they typically do not attempt to identify the causes of these differences. For example, based on the scaling factors in the linear regressions, the CATS AODs are lower than all of the AODs with which they are being compared (i.e., AERONET in Figure 1, MODIS in Figure 2, and CALIOP in Figure 3). This is perhaps not surprising for the AERONET and MODIS comparisons, but the cause for the CATS-CALIOP differences is not as obvious. Differences between CALIOP and MODIS at visible wavelengths are frequently explained by CALIOP’s low daytime detection sensitivity and the missed detection of some of the vertical extent of the aerosol layer (e.g., Kim et al., 2017 and Toth et al., 2018). Can the authors enumerate the possible causes that would explain the disparities between CATS and CALIOP?

*Response: Slopes in linear regressions can often be biased by outliers. In Figure 6, which are spatial plots of AODs from CALIOP and CATS, differences are less noticeable for the DJFMAM season. For the JJASON season, CATS AODs are lower at certain regions (Middle East, India, and North Africa) and higher over other regions (South Africa). The cause of those discrepancies, however, is unclear to us. Also, Version 2 of the CATS data are used in this study, and we expect some difference with the version 3 of CATS data. To really explore the issue, it deserves a paper of its own. Thus, we leave this topic to a future paper.*

Comment: Furthermore, given the lower CATS AODs shown in Figure 2, it's surprising to see that the CATS extinctions coefficients shown in Figure 5 are typically larger than CALIOP at all altitudes, and that the closest agreement is over land (where CATS slightly underestimates CALIOP at lower altitudes). Again, some discussion of the possible causes of this paradox would be welcome.

*Response: First, there is a call from the community to avoid using slopes from the regression analysis as they are prone to noisy data, and we are kind of agree with them. Statistically, we expect a high percentage of small AODs versus large AODs. Still, slopes are dominated by high AOD cases, while the averaged profiles may be more dominated by low AOD cases. This could explain the difference.*

Comment: The results shown in Figure 5 are a prime candidate for further investigation into the underlying causes of the differences. Except for the over land case, CATS extinction profiles consistently and significantly overestimate CALIOP extinction profiles. It seems that there are four likely suspects in causing this (always keeping in mind that that all four could be collaborating in various nefarious ways to bring this about): layer detection, cloud-aerosol discrimination (including inadequate boundary layer cloud clearing), lidar ratio selection, and calibration. Of these four, the easiest to investigate (at least at a superficial level) is lidar ratio. The table below shows the default lidar ratios assigned by each instrument.

Aerosol Type	CATS	CALIOP
Dust	40 sr	44 sr
Dust mixture (a)	40 sr	N/A
Polluted dust (a)	N/A	48 sr
Dusty marine (a)	N/A	37 sr
Marine	25 sr	23 sr
Clean/background	35 sr	30 sr
Polluted continental	35 sr	30 sr
Smoke	40 sr	30 sr
Volcanic (b)	35 sr	44 sr

a) CATS identified dust mixtures over land and water; CALIOP identifies 'polluted dust' over land only and 'dusty marine' over water only.

(b) For CATS, all aerosol above 10 km is classified as volcanic. For CALIOP, volcanic aerosol is identified in the stratosphere only.

Since the CATS marine lidar ratio is large than the CALIOP marine lidar ratio, and the CATS dust mixture lidar ratio is larger than the CALIOP dusty marine lidar ratio (and CATS smoke and polluted continental lidar ratios are greater than their CALIOP counterparts as well), then, *all other things being equal*, one should expect the CATS over-ocean extinction profiles to be uniformly larger than the CALIOP extinction profiles. (But are all other things actually equal?)

The case is less clear over land. But since the CATS dust lidar ratio is less than the CALIOP dust lidar ratio and the CATS dust mixture lidar ratio is less than the CALIOP polluted dust lidar

ratio, if we assume that the over-land aerosols detected in this study are dominated by dust (which might not be a bad assumption?), then perhaps the over-land profile comparison makes sense too. (All other things being equal, that is...)

*Response:*

*We have added a discussion of potential sources of CATS-CALIOP extinction and AOD differences in the text:*

*“In addition, due to the precessing orbit of the ISS, the CATS sampling is irregular and very different compared to the sun-synchronous orbits of the A-Train sensors. These orbital differences between CATS and CALIOP make comparing the data from these two sensors challenging since they are fundamentally observing different locations of the Earth at different times. Thus, we shouldn’t expect the extinction profiles and AOD from these two sensors to completely agree. Additionally, there are other algorithm and instrument differences that can lead to differences in extinction coefficients and AOD. Over land where dust is the dominant aerosol type, differences in lidar ratios between the two retrieval algorithms (CATS uses 40 sr while CALIOP uses 44 sr), can cause CATS extinction coefficients that are up to 10% lower than CALIOP, potentially explaining the higher CALIOP extinction values in Figure 5e. Over ocean, especially during daytime, differences in CATS and CALIOP lidar ratios for marine and smoke aerosols, as well as issues with CATS cloud-aerosol discrimination in V2-01 for daytime observations, can cause CATS extinction coefficients that are as much as 25% higher than CALIOP (Figure 5b and 5d). Yorks et al. (2019) shows examples of these daytime cloud-aerosol discrimination issues in V2-01 data, which have been improved for CATS V3-00 data. A brief analysis using 3 months of CATS V3-00 data showed improvement in agreement for AOD, but some differences were still evident in the extinction vertical profiles. These remaining differences, as well as the differences observed in nighttime only profiles (Figure 5c) are likely attributed to differences in CATS and CALIOP 1064 nm backscatter calibration. Pauly et al. (2019) reports that CATS attenuated total backscatter is about 18% higher than CALIOP due to calibration uncertainties for both sensors.”*

Comment: The CATS extinction profiles shown in Figures 5 and 10 peak at altitudes some hundreds of meters higher than do CALIOP’s, except over land. While CALIOP’s profiles show almost no roll off until about the last range bin above the surface, the CATS profiles start dropping off below about 500 m, or at approximately 8 to 9 range bins above the surface. What is happening here? Is CATS altitude registration and/or surface detection the culprit? Or is the cloud filter too aggressive in the boundary layer (i.e., are strongly scattering aerosols being misclassified as clouds)? Irrespective of the underlying cause(s), is this behavior a major source of AOD differences between CATS and CALIOP?

*Response: The 2 biggest issues in the CATS V2-01 data were the daytime calibration and the daytime cloud-aerosol discrimination. A CATS paper in preparation (Yorks et al., 2019) has included details about the cloud-aerosol discrimination issues, while Rebecca Pauly’s 1064 nm calibration paper has a lot of details about the new daytime calibration. We have checked this*

*issue by reprocessing the analysis using 3 months of V3 data and we found an improvement in agreement for AOD, but with some differences still evident in the vertical profiles.*

Comment: The seasonal maps (Figure 6) show that the CALIOP AODs exceed those of CATS over the Arabian Peninsula, and to a smaller degree over the African region bordering the Gulf of Guinea. Can this also be explained by differences in lidar ratio selection, or are there other factors at work?

*Response: We suspect the difference in retrieval method as mentioned above may contribute. Also, CALIOP provides early morning and afternoon overpasses while CATS can observe at near all solar hours, the differences may also be associated with these sampling differences.*

### **Specific Comments**

Comment: page 4, line 85: provide a reference for “Feature Type Score”

*Response: We have added the reference to the text.*

Comment: page 5, line 107: did the authors also consider potential sources of bias errors; e.g., unusually large or small calibration coefficients, or large values of overlying integrated attenuated backscatter?

*Response: We have adopted the QA steps from a few previous papers such as Campbell et al., 2012; Toth et al., 2016; 2018. The thresholds for the above mentioned criteria are not mentioned and used in those previous papers, and thus we didn't include the check as suggested.*

Comment: page 5, line 113: “Extinction\_Coefficient\_Uncertainty\_1064\_Fore\_FOV  $\leq 10 \text{ km}^{-1}$ ”; despite the heritage from Campbell et al. (2012), using relative uncertainties still makes much, much more sense. Given the noise in the CATS daytime measurements, an uncertainty threshold of  $10 \text{ km}^{-1}$  might be reasonable for an estimated extinction coefficient of  $1 \text{ km}^{-1}$ . However, for the substantially smaller extinction coefficients (e.g.,  $0.01 \text{ km}^{-1}$  to  $0.1 \text{ km}^{-1}$ ) that make up a very large majority of the measurements, an uncertainty threshold of  $10 \text{ km}^{-1}$  seems prohibitively large.

*Response: Agreed. Since we have to apply the thresholds to all observations, lowering the threshold may exclude heavy plumes that may indeed be valid. Also, other QA steps, along with this threshold are also used, as thus, we expect some of the issues as mentioned can be captured by other QA steps. Thus, the QA steps remain unchanged.*

Comment: page 6, line 128: distinguish between laser spot size ( $\sim 70 \text{ m}$ ) and receiver footprint diameter at the Earth's surface ( $\sim 90 \text{ m}$ ).

*Response: We have changed the sentence to “with a laser spot size of around  $70 \text{ m}$ ”*

Comment: page 6, line 129: say which version of the CALIPSO data products was used (version 4.1, right?)

*Response: We have included “CALIOP Level 2.0 Version 4.1” in the sentence.*

Comment: page 7, line 137: “signal-to-noise”, not “single to noise”

*Response: Done.*

Comment: page 7, line 148: “Atmospheric\_Volume\_Description = 3 (aerosol only)”; note that in the CALIPSO version 4.1 data products, 3 indicates tropospheric aerosols and 4 indicates stratospheric aerosols. Were stratospheric aerosols excluded accidentally or deliberately? (Previous versions of the CALIPSO data products did not differentiate between tropospheric and stratospheric aerosols. In these earlier products, requiring the atmospheric volume description to equal 3 would correctly identify all aerosol data.) If accidentally, please correct the calculations. If deliberately, please explain why.

*Response: We have updated this to include Atmospheric\_Volume\_Description = 4 as well, and updated the text accordingly.*

*“Atmospheric\_Volume\_Description = 3 or 4 (aerosol only)”*

Comment: page 8, line 163: logarithmic interpolation, correct? Also, please state the actual value of the Ångström exponent given by Shi et al.

*Response: Yes. The Angstrom exponent value is computed for each AOD retrieval. We have revised the discussion to avoid confusion. “Here we assume the angstrom exponent value, computed using instantaneous AOD retrievals at the 860 and 1240 nm, remains the same for the 860 to 1064 nm wavelength range, similar to what has been suggested by Shi et al., (2011; 2013).”*

Comment: page 8, line 170: while “AERONET data are considered as the ground truth for evaluating CATS retrievals”, it should be noted that there are very few AERONET sites in remote oceans. Do MODIS retrievals substitute as the gold standard in these places?

*Response: Even though a better performance can be expected from MODIS aerosol retrievals over ocean versus over land, we still think that only AERONET data should be used for ground truth, as instantaneous retrievals from passive sensors suffer from various issues such as cloud contamination.*

Comment: page 9, line 186–187: some discussion on the rationale for the choices of  $\pm 0.4^\circ$  and  $\pm 30$  minutes would be helpful in evaluating the strength of the comparisons.

*Responses: We picked this threshold following a few previous papers (e.g. Toth et al., 2018). We have added discussions in the text to further clear this issue:*

*“Note that as suggested by Omar et al., 2013, the choices of spatial and temporal collocation windows have an effect on collocation results. However, we consider this as a topic beyond the scope of this study”*

Comment: page 9, line 193: how frequently do “profiles with all retrieval fill values” occur in the CATS data set?

*Response: We have examined the dataset and found that profiles in which there were no cloud or aerosol made up about 5.4% (3583933/65792363) of all profiles. The text has been updated accordingly.*

*“Such profiles containing all retrieval fill values were found to make up approximately 5.4% of all CATS profiles in the dataset.”*

Comment: page 9, line 194: as a rule of thumb, how close to sunrise and sunset can reliable AERONET measurements be obtained?

*Response: We are not aware if any study have been conducted on this issue. Because it is hard to “validate” AERONET observations. But it is an interesting topic for a future paper.*

Comment: page 11, line 244: The authors say, “using over land (ocean) daytime data only, for a total of 171 (1207) collocated pairs.” Here we echo the remarks of an anonymous reviewer commenting on a paper for which one of us (Mark Vaughan) is a coauthor (see <https://doi.org/10.5194/acp-2018-1090-RC1>).

Way back in 2010 Prof. Robock pleaded with us to end this misuse of parentheses [Robock, A. (2010), Parentheses are (are not) for references and clarification (saving space), Eos Trans. AGU, 91(45), 419–419, doi:10.1029/2010EO450004]. My understanding is that one of the publishers in our field has specifically written it out of their style guide. I read pretty widely and the only genre of writing where I have experienced this application of parentheses is in the atmospheric sciences journals. I hope the authors will consider rewriting this sentence.

*Response: Done. We have rewritten the sentence.*

Comment: page 11, line 245: The authors say, “daytime data from both CALIOP and CATS are expected to be noisier due to solar contamination”. While this is true, the day-night differences at 1064 nm are very different for the two lidars. CATS daytime SNR is substantially worse than CATS nighttime SNR, whereas CALIOP daytime SNR is only marginally worse than CALIOP nighttime SNR. The primary reason for this is that CALIOP 1064 nm detector is an avalanche photodiode for which the dark counts contribute substantial amounts of noise irrespective of the external lighting conditions. Moreover, while CATS 1064 nm nighttime SNR is much higher than CALIOP 1064 nm nighttime SNR, for daytime measurements the CALIOP SNR is higher. This should be explained in greater detail in a forthcoming CATS calibration paper.

*Response: Great comment. But we think those comments should be included in a future paper, hopefully written by one of the coauthors.*

Comment: page 12, line 260: “it is speculated”. Who’s doing this speculating? If it’s the authors, then come right out and say so!

*Response: We have revised the sentence to “although we speculate”*

Comment: page 14, line 311: The authors say, “the shapes of the CATS and the CALIOP nm extinction vertical profile are very similar for all three cases”. This qualitative assessment would be much more meaningful if it was augmented by a set of quantitative metrics (e.g., profiles of  $(CATS(z) - CALIOP(z)) / CALIOP(z)$ , with error bars to indicate the magnitude of the variability in the ratios).

*Response: We have included a plot of  $CATS(z) - CALIOP(z)$  (Appendix A) for the mean CATS and CALIOP vertical profiles. As CALIOP extinction values become very small, the ratio of  $(CATS(z) - CALIOP(z)) / CALIOP(z)$  has a tendency to grow very large from just a few data points and greatly impacts the standard deviation. Thus we plotted only the difference and did not include  $(CATS(z) - CALIOP(z)) / CALIOP(z)$  with error bars with this particular plot.*

Comment: page 18, line 405: The authors say, “nighttime retrievals from CATS *are considered to be less noisy than daytime*” (emphasis added). This sentence suggests that there might be some debate about day versus night noise magnitudes. There is no such debate. The fact is that “nighttime retrievals from CATS *are significantly and demonstrably less noisy than daytime retrievals*”.

*Response: We have used the wording as suggested. Thanks for the comment.*

Comment: page 23, lines 514–517: The authors’ conclusions reinforce the conventional wisdom. However, we think it’s important to emphasize that at present these conclusions are highly tentative, and will remain so until a comprehensive analysis of the CATS calibration accuracy and stability is completed.

*Response: We have added the comment as suggested:*

*“Still, at present these conclusions are tentative, and will remain so until a comprehensive analysis of the CATS calibration accuracy and stability is completed. “*

1  
2  
3  
4  
5  
6  
7  
8  
9  
10  
11  
12  
13  
14  
15  
16  
17  
18  
19  
20  
21  
22  
23  
24  
25

**Investigation of CATS aerosol products and application toward global diurnal variation of aerosols**

Logan Lee<sup>1</sup>, Jianglong Zhang<sup>1</sup>, Jeffrey S. Reid<sup>2</sup>, and John E. Yorks<sup>3</sup>

<sup>1</sup>Department of Atmospheric Sciences, University of North Dakota, Grand Forks, ND

<sup>2</sup>Marine Meteorology Division, Naval Research Laboratory, Monterey, CA

<sup>3</sup>NASA Goddard Space Flight Center, Greenbelt, MD

Submitted to

ACP

Dec. 2018

Corresponding Author: [jzhang@atmos.und.edu](mailto:jzhang@atmos.und.edu); [logan.p.lee@und.edu](mailto:logan.p.lee@und.edu)

26  
27  
28  
29  
30  
31  
32  
33  
34  
35  
36  
37  
38  
39  
40  
41  
42  
43  
44  
45  
46

### **Abstract**

We present a comparison of 1064 nm aerosol optical depth (AOD) and aerosol extinction profiles from the Cloud-Aerosol Transport System (CATS) Level 2 aerosol product with collocated Aerosol Robotic Network (AERONET) AOD, Aqua and Terra Moderate Imaging Spectroradiometer (MODIS) Dark Target (AOD) and Cloud-Aerosol Lidar with Orthogonal Polarization (CALIOP) AOD and extinction data for the period of Feb. 2015-Oct. 2017. Upon quality assurance checks of CATS data, reasonable agreements are found between aerosol data from CATS and other sensors. Using quality assured CATS aerosol data, for the first time, variations in AODs and aerosol extinction profiles are evaluated at 00, 06, 12, and 18 UTC (and/or 0:00 am, 6:00 am, 12:00 pm and 6:00 pm local solar times) on both regional and global scales. This study suggests that marginal variations are found in AOD from a global mean perspective, with the maximum and minimum aerosol vertical profiles found at local noon and 6:00 pm local time respectively, for both the June-November and December-May seasons. Strong diurnal variations are found over North Africa and India for the December-May season, and over North Africa, Middle East, and India for the June-November season. In particular, over North Africa, during the June-November season, a diurnal peak in aerosol extinction profile of 20% larger than daily mean is found at 6:00 am (early morning local time), which may possibly be associated with dust generation through the breaking down of low level jet during morning hours.

47 **1.0 Introduction**

48 Aerosol measurement through the sun-synchronous orbits of Terra and Aqua by nature  
49 encourages a larger scale, daily average point of view. Yet, we know that pollution (e.g., Zhao et  
50 al., 2009; Tiwarl et al., 2013; Kaku et al., 2018), fires and smoke properties (e.g., Reid et al.,  
51 1999; Giglio et al., 2003; Hyer et al., 2013), and dust (e.g., Mbourou, et al., 1997; Fielder et al.,  
52 2013; Heinold et al., 2013) can exhibit strong diurnal behavior. Sun-synchronous passive  
53 satellite aerosol observations from the solar spectrum only provide a small sampling of the full  
54 diurnal cycle and geostationary sensors such as the Advanced Himawari Imager (AHI) on  
55 Himawari 8 (Yoshida et al., 2018) and Advanced baseline Imager on GOES-16/17 (Aerosol  
56 Product Application Team of the AWG Aerosols/Air Quality/Atmospheric Chemistry Team,  
57 2012) satellites, while an improvement over their predecessors, must overcome the broader range  
58 of scattering and zenith angles (Wang et al., 2003; Christopher and Zhang, 2002) with no  
59 nighttime retrievals. AEROSOL ROBOTIC NETWORK (AERONET; Holben et al., 1998) based sun  
60 photometer studies improve sampling, but until very recently with the development of a  
61 prototype lunar photometry mode, are also limited to daylight hours. The critical early morning  
62 and evening are largely missed in solar observation based approaches.

63 Observation-based diurnal variations of aerosol properties are needed for improving  
64 chemical transport modeling, geochemical cycles and ultimately climate. The measurement of  
65 diurnal variations of aerosol properties resolved in the vertical is especially crucial of aerosol  
66 phenomena for visibility and particulate matter forecasts. Indeed, the periods around sunrise and  
67 sunset show significant near surface variability that is difficult to detect with passive sensors.  
68 While lidar data from Cloud-Aerosol Lidar with Orthogonal Polarization (CALIOP) provide

69 early afternoon and morning observations, two temporal points and a 16 day repeat cycle are  
70 insufficient to evaluate the morning and evening hours.

71 Some of the limiting factors in previous studies can be addressed by the Cloud-Aerosol  
72 Transport System (CATS) lidar flying aboard the International Space Station (ISS) since 2015  
73 (McGill et al. 2015). The ISS's precessing orbit with a  $51.6^\circ$  inclination allows for 24 hour  
74 sampling of the tropics to mid-latitudes, with the ability to observe aerosol and cloud vertical  
75 distributions at both day and night time with high temporal resolution. For a given location  
76 within  $\pm 51.6^\circ$  (Latitude), after aggregating roughly 60 days of data, near full diurnal cycle of  
77 aerosol and cloud properties can be obtained from CATS observations (Yorks et al. 2016). This  
78 provides a new opportunity for studying diurnal variations (day and night) in aerosol vertical  
79 distributions from space observations.

80 Use of CATS has its own challenges. Most importantly, CATS retrievals must cope with  
81 variable solar noise around the terminator where we expect the strongest diurnal variability to  
82 exist. Further, CATS lost its 532 nm channel early in its deployment, leaving only a 1064 nm  
83 channel functioning. The availability of only one wavelength limited the CATS cloud-aerosol  
84 discrimination algorithm, which can cause a loss of accuracy compared to CALIPSO which has  
85 2 wavelengths. This deficiency is in part overcome by using the Feature Type Score [\(CATS](#)  
86 [Algorithm Theoretical Basis Document\)](#). Using two years of observations from CATS, in this  
87 paper, we focus on understanding of the following questions: How well do CATS derived  
88 aerosol optical depth (AOD) and aerosol vertical distributions compare with aerosol properties  
89 derived from other ground-based and satellite observations such as AERONET, MODIS and  
90 CALIOP? Do differences exhibit a diurnal cycle? What are the diurnal variations of aerosol

Formatted: Font: (Default) Times New Roman, 12 pt

91 optical depth on a global domain? What are the diurnal variations of aerosol vertical distribution  
92 on both regional and global scales?

93

## 94 **2.0 Datasets**

95 Four datasets, including ground-based AERONET data, as well as satellite retrieved  
96 aerosol properties from MODIS and CALIOP, are used for inter-comparing with AOD and  
97 aerosol vertical distributions from CATS. Upon thorough evaluation and quality assurance  
98 procedures, CATS data are further used for studying diurnal variations of AOD and aerosol  
99 vertical distributions for the period of Feb. 2015 – Oct. 2017.

100

## 101 **2.1 CATS**

102 CATS Level 2 (L2) Version 2-01 5 km Aerosol Profile products (L20\_D-M7.2-V2-  
103 01\_5kmPro, L20\_N-M7.2-V2-01\_5kmPro) were used in this study for the entire period of CATS  
104 operation on the ISS (~Feb. 2015–Oct. 2017). CATS L2 profile data are provided at 5 km along-  
105 track horizontal resolution and 533 vertical levels at 60 m vertical resolution and a wavelength of  
106 1064 nm. CATS also provides data at 532 nm, but due to a laser-stabilization issue, 532 nm data  
107 is not recommended for use (Yorks et al. 2016). Thus, only 1064 nm products were used in this  
108 study. CATS data are quality-assured following a manner similar to Campbell et al. (2012),  
109 which was applied to CALIOP. QA thresholds (including extinction QC flag, Feature Type  
110 Score, and uncertainty in extinction coefficient) are listed below:

111 (a) Extinction\_QC\_Flag\_1064\_Fore\_FOV is equal to 0

112 (b) Feature\_Type\_Fore\_FOV = 3 (aerosol only)

113 (c)  $-10 \leq \text{Feature\_Type\_Score\_FOV} \leq -2$

Deleted: ; Yorks et al. 2015

115 (d) Extinction\_Coefficient\_Uncertainty\_1064\_Fore\_FOV  $\leq 10 \text{ km}^{-1}$

116 Extinction was also constrained using a threshold as provided in the CATS data catalog  
117 (Extinction\_Coefficient\_1064\_Fore\_FOV  $\leq 1.25 \text{ km}^{-1}$ ), similar to several previous studies  
118 (Redemann et al., 2012; Toth et al., 2016). Only profiles with extinction coefficient values less  
119 than  $1.25 \text{ km}^{-1}$  are included in this study. Small negative extinction coefficient values, however,  
120 are included in aerosol profile related analysis, to reduce potential high biases in computed mean  
121 profiles. Note that a similar approach has also be conducted in deriving passive-based AOD  
122 climatology (e.g. Remer et al., 2005). For this study, both the  
123 Aerosol\_Optical\_Depth\_1064\_Fore\_FOV and Extinction\_Coefficient\_1064\_Fore\_FOV datasets  
124 were used to provide AOD and 1064 nm extinction profiles (hereafter the term “extinction” will  
125 refer to 1064 nm unless explicitly stated otherwise), respectively.

126

## 127 2.2 CALIOP

128 NASA’s CALIOP is an elastic backscatter lidar that operates at both 532 nm and 1064  
129 nm wavelengths (Winker et al., 2009). Being a part of the A-Train constellation (Stephens et al.,  
130 2002), CALIOP provides both day- and night-time observations of Earth’s atmospheric system,  
131 at a sun-synchronous orbit, with a laser spot size of around 70 m and a temporal resolution of  
132 ~16 days (Winker et al., 2009). For this study, CALIOP Level 2.0 Version 4.1 5 km Aerosol  
133 Profile products (L2\_05kmAProf) are used for inter-comparing to CATS retrieved AODs and  
134 aerosol vertical distributions.

135 L2\_05kmAProf data are available at 5 km horizontal resolution along-track and include  
136 aerosol retrievals at both 532 nm and 1064 nm wavelengths. The vertical resolution is 60 m  
137 near-surface, degrading to 180 m above 20.2 km in MSL altitude. As only 1064 nm CATS data

**Deleted:** to the nominal range

**Deleted:**  $0 \leq$

**Deleted:**

**Formatted:** Superscript

**Deleted:** Due to the presence of a large amount of near zero negative extinction values, profiles containing these values were also considered by setting all near zero negative values to zero, resulting in an effective threshold of Extinction\_Coefficient\_1064\_Fore\_FOV  $\leq 1.25 \text{ km}^{-1}$ .

**Formatted:** Font: 12 pt

**Deleted:** narrow swath

**Deleted:** increasing

148 are used in this study as mentioned above, likewise only those CALIOP parameters relating to  
149 1064 nm are used in this study (Vaughan et al., 2018; Omar et al., 2013). Note that as suggested  
150 by Rajapakshe et al. (2017), lower signal-to-noise ratio (SNR) and higher minimum detectable  
151 backscatter are found for the CALIOP 1064 nm data in-comparing with the CALIOP 532 nm  
152 data. Also, the CALIOP aerosol layers are detected at 532 nm and the 1064 nm extinction is  
153 only computed for the bins within these layers. This may introduce a bias for aerosol above  
154 cloud studies. In this study, Extinction\_Coefficient\_1064 and  
155 Column\_Optical\_Depth\_Tropospheric\_Aerosols\_1064 are used for CALIOP extinction and  
156 AOD retrievals, respectively (Vaughan et al., 2018; Omar et al., 2013). As with the CATS data,  
157 CALIOP data are quality-assured following the quality assurance steps as mentioned in a few  
158 previous studies (e.g. Campbell et al., 2012; Toth et al., 2016; 2018). These QA thresholds are  
159 listed below:

Deleted: single to noise

- 160 (a) Extinction\_QC\_Flag\_1064 is equal to 0,1,2,16, or 18  
161 (b) Atmospheric\_Volume\_Description = 3 or 4 (aerosol only)  
162 (c) -100 <= CAD\_Score <= -20  
163 (d) Extinction\_Coefficient\_Uncertainty\_1064 <= 10  $km^{-1}$

164 Furthermore, as in Campbell et al. (2012), only those profiles with AOD > 0 were  
165 retained in order to avoid profiles composed of only retrieval fill values. Extinction was also  
166 constrained to the nominal range provided in the CALIOP data catalog (Extinction\_1064 <= 1.25  
167  $km^{-1}$ ), similar to our QA procedure for CATS as described above.

168

### 169 **2.3 MODIS Collection 6.1 Dark Target product**

171 Moderate Resolution Imaging Spectroradiometer (MODIS) Aqua and Terra Collection  
172 6.1 Dark Target over-ocean AOD data (Levy et al., 2013) were used for comparison to CATS  
173 AOD. The data field of “Effective\_Optical\_Depth\_Best\_Ocean” were used and only those data  
174 flagged as “good” or “very good” by the Quality\_Assurance\_Ocean runtime QA flags are  
175 selected for this study, similar to Toth et al. (2018). Because MODIS does not provide AOD in  
176 the 1064 nm wavelength, AOD retrievals from 860 and 1240 nm spectral channels are used to  
177 logarithmically interpolate AODs at 1064 nm. Here we assume the angstrom exponent value,  
178 computed using instantaneous AOD retrievals at the 860 and 1240 nm, remains the same for the  
179 860 to 1064 nm wavelength range, similar to what has been suggested by Shi et al., (2011;  
180 2013). Only totally cloud free (or cloud fraction equal to zero) retrievals, as indicated by the  
181 Cloud\_Fraction\_Land\_Ocean parameter are used.

Deleted: , assuming a constant

Deleted: as

182

#### 183 **2.4 AERONET**

184 By measuring direct and diffuse solar energy, AERONET observations are used for  
185 retrieving AOD and other ancillary aerosol properties such as size distributions (Holben et al.,  
186 1998). AERONET data are considered as the ground truth for evaluating CATS retrievals in this  
187 study. Only cloud screened and quality assured version 3 level 2 AERONET data at the 1020  
188 nm spectrum are selected and are used for inter-comparing with CATS AOD retrievals at the  
189 1064 nm wavelength. AERONET does not have specific guidance on error in the 1020 nm  
190 channel, as it is known to have some thermal sensitivities. However they do report significantly  
191 more confidence in version 3 of the data, which has temperature correction (Giles et al., 2018).  
192 Error models are ongoing, and for this study we assume double the RMSE, or +/-0.03.

193

196 **3.0 Results & Discussion**

197 **3.1 Inter-comparison of CATS data with AERONET, MODIS and CALIOP data**

198 Note that most evaluation efforts for passive- and active-based AOD retrievals are  
199 focused on the visible spectrum and the performance of AOD retrievals at the 1064 nm channel  
200 is less explored. Thus, in this sub-section, the performance of over land and over ocean CATS  
201 AOD retrievals are compared against AERONET and C6.1 over ocean MODIS DT aerosol  
202 products. In AOD related studies, CAT and CALIOP reported AOD values are used. However,  
203 although not derived in this study, only AOD values with corresponding aerosol vertical  
204 extinction that meet the QA criteria as mentioned in Sections 2.1 and 2.2 were used. CATS  
205 derived aerosol extinction vertical distributions are also cross-compared against collocated  
206 CALIOP aerosol extinction vertical distributions.

Deleted: 1

207  
208 **3.1.1 CATS-AERONET**

209 As the initial check, CATS data from Feb. 2015-Oct. 2017 are spatially (within 0.4  
210 degree Latitude and Longitude) and temporally ( $\pm 30$ minutes) collocated against ground-based  
211 AERONET data. Note that one AERONET measurement may be associated with several CATS  
212 retrievals in both space and time, and vice versa. Thus, both CATS and AERONET data are  
213 further averaged spatially and temporally, which results in only one pair of collocated and  
214 averaged CATS and AERONET data for a given collocated incident. Also, only data pairs with  
215 AOD larger than 0 from both instruments are used for the analysis. This step is necessary to  
216 exclude CATS profiles with all retrieval fill values as discussed in Section 2 (Toth et al., 2018).  
217 Such profiles containing all retrieval fill values were found to make up approximately 5.4% of all

219 [CATS profiles in the dataset.](#) Note that the CATS-AERONET comparisons are for daytime  
220 only, and higher uncertainties are expected for CATS daytime than night AODs.

221 As shown in Figure 1a, without quality-assurance procedures, high spikes in CATS AOD  
222 of above 1 (1064 nm) can be found for collocated AERONET data with AOD less than 0.3 (1020  
223 nm). Those high spikes in CATS AOD may due to cloud contamination in the V2-01 CATS  
224 daytime data, which will be improved in the upcoming CATS V3-00 data products. Upon  
225 completion of the QA steps as outlined in Section 2.1, a reasonable agreement is found between  
226 quality-assured CATS (1064 nm) vs. AERONET (1020 nm) AODs with a correlation of 0.64  
227 (Figure 1b). Comparing Figure 1a with 1b, with the loss of only ~10% of collocated pairs due to  
228 the QA procedures, we have observed an overall improvement in correlation between CATS and  
229 AERONET AOD from 0.17 to 0.64. Note that similar results are found in comparisons between  
230 collocated CATS and MODIS/CALIOP data without the use of QA procedures on CATS data.  
231 Thus, only QAed CATS data are used hereafter. Still, this exercise highlights the need for  
232 careful quality checks of the CATS data before applying the CATS data for advanced  
233 applications to overcome cloud-aerosol discrimination uncertainties.

234

### 235 **3.1.2 CATS-MODIS**

236 To examine over ocean performance, column integrated CATS AODs are inter-compared  
237 with collocated Terra and Aqua C6.1 MODIS DT over ocean AOD, interpolated to 1064 nm.  
238 Over ocean C6.1 MODIS DT data are selected due to the fact that higher accuracies are reported  
239 for over ocean versus over land MODIS DT AOD retrievals (Levy et al., 2013). In addition,  
240 comparing with over land MODIS DT data, which provides AOD retrievals at three discrete  
241 wavelengths (0.46, 0.55 and 0.65  $\mu\text{m}$ ), over water AOD retrievals are available from 7

242 wavelengths including the 0.87 and 1.24  $\mu\text{m}$  spectral channels, allowing a comparison with  
243 CATS AOD at the same wavelength upon interpolation.

244 MODIS and CATS AOT retrievals are collocated for the study period of Feb. 2015-Oct.  
245 2017 (Figure 2). Pairs of CATS and MODIS data were first selected for both retrievals that fall  
246 within  $\pm 30$  minutes and 0.4 degrees latitude and longitude of each other. Then, similar to the  
247 AERONET and CATS collocation procedures, collocated pairs were further averaged to  
248 construct one pair of collocated MODIS and CATS data for a given collocation incident. Shown  
249 in Figure 2a, a correlation of 0.71 is found between collocated over water Terra MODIS C6.1  
250 DT and CATS AODs with a slope of 0.78. Similar results are found for the comparisons  
251 between over water Aqua MODIS and CATS AODs with a correlation of 0.75 and a slope of  
252 0.79.

253

### 254 3.1.3 CATS-CALIOP AOD

255 In the previous two sections, AODs from CATS are inter-compared with retrievals from  
256 passive-based sensors such as MODIS and AERONET. In this section, AOD data from  
257 CALIOP, which is an active-based sensor, are evaluated against AOD retrievals from CATS.  
258 Again, for each collocation incident, pairs of CALIOP and CATS data are selected in which both  
259 retrievals fall within  $\pm 30$  minutes temporally and 0.4 degrees latitude and longitude spatially.  
260 There could be multiple CATS retrievals corresponding to one CALIOP data point, and vice  
261 versa. Thus, the collocated pairs are further averaged in such a way that only one pair of  
262 collocated CATS and CALIOP data is derived for each collocation incident. Note that as  
263 suggested by Omar et al., (2013), the choices of spatial and temporal collocation windows have an  
264 effect on collocation results. However, we consider this as a topic beyond the scope of this study.

Formatted: Font: Not Italic

Formatted: Font: Not Italic

Formatted: Font: Not Italic

Formatted: Font: Not Italic

265 Figure 3a shows the comparison of CATS and CALIOP AODs for all collocated pairs  
266 including both day- and night-time. A reasonable correlation of 0.7, with a slope of 0.69, is  
267 found for a total of 2681 collocated data pairs. Further breaking down the comparison into day  
268 and night cases, a much better agreement is found between the two datasets during nighttime  
269 with a correlation of 0.84 and 0.81 for over-ocean and over-land cases respectively. In  
270 comparison, a lower correlation of 0.62, with a slope of 0.44, is found between the two datasets,  
271 using over land daytime data only, for a total of 171 collocated pairs. Correspondingly, a lower  
272 correlation of 0.52, with a slope of 0.63, is found between the two datasets, using over ocean  
273 daytime data only, for a total of 1207 collocated pairs. This result is not surprising as daytime  
274 data from both CALIOP and CATS are expected to be noisier due to solar contamination (e.g.  
275 Omar et al., 2013; Toth et al., 2016).

276 Still, larger discrepancies between CATS and CALIOP AODs during daytime indicate  
277 that both sensors are more susceptible to solar contamination. To overcome solar contamination  
278 and more accurately detect aerosol layers, CALIOP and CATS data products are averaged up to  
279 80 km and 60 km, respectively. Noel et al. (2018) found that clouds screened using the feature  
280 type score were accurately detected by CATS data products throughout the diurnal envelope of  
281 solar angles. To ensure the solar contamination does not introduce a diurnal bias in aerosol  
282 detection or products, CATS AODs are further evaluated as a function of local time. For each  
283 CATS observation of a given location and UTC time, the associated local time is computed by  
284 adding (subtracting) the UTC time by 1 hour per 15° Longitude away from the Prime Meridian  
285 in the east (west) direction. Figure 4a shows the CATS AOD versus local time for both global  
286 land and oceans. While noisy in data, an averaged AOD peak is found around local noon that is  
287 about 0.02-0.03 higher than both sunrise and sunset times. Still, for high AOD cases, no

Deleted: (0.52)

Deleted: (0.63)

Deleted: (ocean)

Deleted: (1207)

292 significant solar noon peak is found. Also, no major deviations in AODs are found during either  
293 sunrise or sunset time, although ~~we~~ speculate that larger uncertainties in CATS AODs and  
294 extinctions may ~~be present~~ around day and night terminators. Figure 4b shows a similar plot as  
295 Figure 4a, but with the region restricted to 25°S-52°S. Here, we want to investigate the  
296 variations in CATS AODs as a function of local time, over relatively aerosol free oceans. We  
297 picked 25°S as the cutoff line as CATS data only available to 51.6°S (limited to the ISS  
298 inclination angle) and thus, this threshold is used to ensure enough data samples in the analysis,  
299 although some land regions are also included. As indicated in Figure 4b, a clear diurnal variation  
300 is found, with the ~~mean AOD values~~ of 0.07-0.08 found ~~between late morning and early~~  
301 ~~afternoon~~ and smaller AOD values of 0.06 found for both sunrise and sunset times. Also, no  
302 significant deviations in pattern are found for both sunrise and sunset time, plausibly indicating  
303 that solar contamination, as speculated, may not be as significant. It is, however, unclear if the  
304 0.02 AOD difference between local noon and sunrise and sunset times is introduced by retrieval  
305 bias or indeed a physical existence.

306 To further explore the 0.02 difference, Figure 4c shows the difference between  
307 AERONET (1020 nm) and CATS (1064 nm) AOD ( $\Delta$ AOD) as a function of local time, again,  
308 although data are rather noisy, no major pattern is found near sunrise or sunset times, again,  
309 further indicating that solar contamination during dawn or dusk times, may have a less severe  
310 impact to CATS AOD retrievals from a long term mean perspective.

311 In summary, Sections 3.1.1-3.1.3 suggest that with careful QA procedures, AOD  
312 retrievals from CATS are comparable to those from other existing sensors such as AERONET,  
313 MODIS, and CALIOP at the same local times.

314

Deleted: it is

Deleted: d

Deleted: be presente

Deleted: d

Deleted: peak

Deleted: around local noon

321 **3.1.4 CATS-CALIOP Vertical Extinction Profiles**

322 One advantage of CATS is its ability to retrieve both column-integrated AOD and  
323 vertical distributions of aerosol extinction. Therefore, in this section, extinction profiles from  
324 CATS are compared with that from CALIOP. Again, similar to the Section 3.1.3, collocated  
325 profiles for CATS and CALIOP are first found for both retrievals that are close in space and time  
326 (within  $\pm 30$  minutes and 0.4 degrees latitude and longitude). However, different from Section  
327 3.1.3, only one pair of collocated CATS and CALIOP profiles, which has the closest Euclidian  
328 distance on the earth's surface, is retained for each collocated incident.

329 The CATS cloud-aerosol discrimination (CAD) algorithm is a multidimensional  
330 probability density function (PDF) technique that is based on the CALIPSO algorithm (Liu et al.  
331 2009). The PDFs were developed based on Cloud Physics Lidar (CPL) measurements obtained  
332 during over 11 field campaigns and 10 years. Figure 5 shows that CATS V2-01 aerosol  
333 extinction agrees very well with CALIOP for nighttime (Figure 5c) and over land (Figure 5e).  
334 However, CATS overestimates aerosol extinction around 1 km compared to CALIOP during  
335 daytime (Figure 5b) and over ocean (Figure 5d). [This can also be seen on a plot of the difference](#)  
336 [between CATS and CALIOP 1064 nm extinction for all collocated profiles, included in](#)  
337 [Appendix A, where there is an overall positive difference around 1 km.](#) Based on statistical  
338 comparisons of CATS L2O V2-01 cloud and aerosol detection frequencies with CALIOP, it was  
339 determined that, during daytime over ocean, depolarizing liquid water clouds in the lower  
340 troposphere are sometimes classified as lofted dust mixture or smoke aerosols in the CATS V2-  
341 01 data products. This is primarily a result of enhanced depolarization ratios within liquid water  
342 clouds due to multiple scattering (which is not represented in the CPL measurements used for the  
343 PDFs). To overcome this issue, the CATS V3-00 CAD algorithm uses horizontal persistence

Deleted: relative to CALIOP 1064 nm extinction f

Deleted: as shown in Figure 14

Deleted: relative

347 tests and additional tests using variables such as the perpendicular ATB, to better differentiate  
348 clouds and aerosols. More details will be provided in an upcoming paper (Yorks et al., in prep).  
349 Since the CATS V3-00 data has not been released yet, we will focus our discussion of aerosol  
350 diurnal variability on regions primarily over land.

351 In addition, due to the precessing orbit of the ISS, the CATS sampling is irregular and  
352 very different compared to the sun-synchronous orbits of the A-Train sensors. These orbital  
353 differences between CATS and CALIOP make comparing the data from these two sensors  
354 challenging since they are fundamentally observing different locations of the Earth at different  
355 times. Thus, we shouldn't expect the extinction profiles and AOD from these two sensors to  
356 completely agree. Additionally, there are other algorithm and instrument differences that can  
357 lead to differences in extinction coefficients and AOD. Over land where dust is the dominant  
358 aerosol type, differences in lidar ratios between the two retrieval algorithms (CATS uses 40 sr  
359 while CALIOP uses 44 sr), can cause CATS extinction coefficients that are up to 10% lower  
360 than CALIOP, potentially explaining the higher CALIOP extinction values in Figure 5e. Over  
361 ocean, especially during daytime, differences in CATS and CALIOP lidar ratios for marine and  
362 smoke aerosols, as well as issues with CATS cloud-aerosol discrimination in V2-01 for daytime  
363 observations, can cause CATS extinction coefficients that are as much as 25% higher than  
364 CALIOP (Figure 5b and 5d). Yorks et al. (2019) shows examples of these daytime cloud-aerosol  
365 discrimination issues in V2-01 data, which have been improved for CATS V3-00 data. A brief  
366 analysis using 3 months of CATS V3-00 data showed improvement in agreement for AOD, but  
367 some differences were still evident in the extinction vertical profiles. These remaining  
368 differences, as well as the differences observed in nighttime only profiles (Figure 5c) are likely  
369 attributed to differences in CATS and CALIOP 1064 nm backscatter calibration. Pauly et al.

370 (2019) reports that CATS attenuated total backscatter is about 18% higher than CALIOP due to  
371 calibration uncertainties for both sensors.

372 CATS also has a stronger extinction when compared to CALIOP in the lowest 2 km,  
373 which may be due to differences in cloud screening. Vertical profiles of collocated CATS and  
374 CALIOP extinction for daytime only profiles and nighttime only profiles are shown in Figure 5b  
375 and 5c, respectively. Compared to a total collocated pair count of 2681 in the overall profile  
376 data, day and night profiles have 1342 and 1339 collocated pairs, respectively. Again, the shapes  
377 of the CATS and the CALIOP nm extinction vertical profile are very similar for all three cases,  
378 despite the above mentioned offsets in altitude. Figure 5d and 5e show the mean of those  
379 extinction profiles which occurred over-water and over-land, as defined by the CATS surface  
380 type flag. Again in both cases CATS and CALIOP have very similar shapes in their vertical  
381 extinction profiles. The vertical structure of over-water extinction is also very similar to that of  
382 all profiles, day, and night, which is perhaps not surprising as water profiles made up 2111 of  
383 2681 (~79%) collocated pairs. The vertical structure of over-land is more different than the other  
384 groups, as the extinction is higher throughout a larger depth of the atmosphere, tapering off much  
385 more slowly from the surface. Furthermore, the extinction from CATS is actually lower than  
386 CALIOP for over-land profiles, unlike all other categories.

### 387 388 **3.2 Diurnal Cycle of AODs and Aerosol Vertical Distributions**

389 Using the QAed CATS data, seasonal variations as well as diurnal variations in CATS  
390 AODs are derived in this section. Diurnal variations in the vertical distributions of CATS aerosol  
391 extinction are also examined at both global and regional scales.

392

393 **3.2.1 Seasonal and Diurnal Variation of AOD**

394 Figures 6a-b show the spatial distributions of CATS AODs at the 1064 nm spectral  
395 channel for boreal winter-spring (Dec.-May, DJFMAM) and boreal summer-fall (June-Nov,  
396 JJASON) seasons, for the period of Feb. 2015-Oct. 2017. To construct Figures 6a and 6b,  
397 quality-assured CATS AODs are first binned on a 5 degree by 5 degree grid over the globe for  
398 the above mentioned two bi-seasons. For each  $5 \times 5^\circ$  (Latitude/Longitude) bin, for a given  
399 season, CATS AODs are averaged on a pass-basis first, and then further averaged seasonally to  
400 represent AOD value of the given bin.

401 In DJFMAM season, significant aerosol features are found over North Africa, Mid-East,  
402 India and Eastern China. For the JJASON season, besides the above mentioned regions, aerosol  
403 plumes are also observable over Southern Africa, related to summer biomass burning of the  
404 region (e.g. Eck et al., 2013). The seasonal-based spatial distributions of AODs from CATS,  
405 although reported at the 1064 nm channel which is different from the 550 nm channel that is  
406 conventionally used, are similar to some published results (e.g. Lynch et al., 2016).

407 For comparison purposes, Figures 6c-6d shows similar plots as Figures 6a-6b, but with  
408 the use of CALIOP AOD at the 1064 nm spectral channel. Note that those are climatological  
409 means rather than pairwise comparisons. While patterns are similar in general, at regions with  
410 peak AODs of 0.4 or above for CALIOP, such as North Africa for the DJFMAM season and  
411 North Africa, Middle-East and India for the JJASON, much lower AODs are found for CATS.  
412 In some other regions, such as over South Africa and upper-portion of Middle-East for the  
413 JJASON season, however, higher CATS AOD values are observed. [A table of mean AOD](#)  
414 [across each of these regions as well as over the globe \(within the latitude range where CATS has](#)  
415 [data\) has been included for reference \(Table 2\).](#) Figures 6e and 6f show the similar spatial plots

416 as Figures 6a and 6b but with the use of Aqua MODIS AODs from the DT products. For the  
417 Aqua MODIS DT products, aerosol retrievals at the short-wave Infra-red channels are only  
418 available over oceans, and thus Figures 6e-6f show only over ocean retrievals. Again, while  
419 general AOD patterns look similar, discrepancies are also visible, such as over the coast of south  
420 east Africa for the JJASON season. Those discrepancies may result from biases in each product,  
421 but it is also possibly due to the differences in satellite overpass times, as CALIOP provides  
422 early morning and afternoon over passes, and Aqua MODIS has an over pass time after local  
423 noon. while CATS is able to report atmospheric aerosol distributions at multiple times during a  
424 day. It is also possibly due to aerosol above cloud related issues as reported by Rajapakshe et al.  
425 (2017), as explained in Section 2.2.

Deleted: both MODIS and

426 Similar to Figures 6a and 6b, Figures 7a and 7b show the spatial distribution of CATS  
427 AODs, but for CATS extinction values that are below 1 km Above Ground Level (AGL) only,  
428 for the DJFMAM and JJASON seasons respectively. Figure 7c and 7d (7e and 7f) show the  
429 CATS mean AOD plots for extinction values from 1-2 km AGL (> 2 km AGL). For the  
430 DJFMAM season, elevated aerosol plumes with altitude above 2 km AGL are found over the  
431 North coast of Africa. For the JJASON season, elevated dust plumes (> 2 km AGL) are found  
432 over North Africa and the Middle-East regions, while elevated smoke plumes are found over the  
433 west coast of South Africa where above cloud smoke plumes are often observed during the  
434 Northern hemispheric summer season (e.g. Alfaro-Contreras et al., 2016).

Deleted: AGL

435 CATS has a non-sun-synchronized orbit, which enables measurements at near all solar  
436 angles. Thus, we also constructed  $5 \times 5^\circ$  (Latitude/Longitude) gridded seasonal averages (for  
437 DJFMAM and JJASON seasons) of CATS AODs at 0, 6, 12 and 18 UTC that represent 4 distinct  
438 times in a full diurnal cycle, as shown in Figure 8. To construct the seasonal averages,

441 observations within  $\pm 3$  hours of a given UTC time as mentioned above are averaged to represent  
442 AODs for the given UTC time. On a global average, the mean AODs are 0.090, 0.090, 0.090  
443 and 0.091 for 0, 6, 12 and 18 UTC respectively for the JJASON season and are 0.101, 0.100,  
444 0.097 and 0.097 for the DJFMAM season. Thus, no significant diurnal variations are found on a  
445 global scale, as global means are dominated by background aerosols that have weak diurnal  
446 variations in measured absolute AOD values.

447 Still, strong diurnal variations with the maximum averaged diurnal AOD changes of  
448 above 0.15 can be observed for regions with significant aerosol events such as Northern Africa  
449 and India for the DJFMAM season and Northern Africa, Southern Africa, Mid-East and India for  
450 the JJASON season, as illustrated in Figure 9. Note that Fig. 9a (9b) shows the maximum minus  
451 minimum seasonal mean AODs for the four difference times as shown in Figs. 8a,c,e,g  
452 (8b,d,f,h). Interestingly but not unexpectedly, regions with maximum diurnal variations match  
453 well with locations of heavy aerosol plumes as shown in Figures 6 and 8.

454

### 455 **3.2.2 Diurnal variations of Aerosol Extinction on a Global Scale (both at UTC and local** 456 **time)**

457 Using quality-assured CATS derived aerosol vertical distributions, mean global CATS  
458 extinction vertical profiles are also generated as shown in Figure 10. Similar to steps as  
459 described in the section 3.2.1, CATS extinction profiles are binned into 00, 06, 12, and 18 UTC  
460 times based on the closest match in time for the JJASON and DJFMAM seasons. Figure 10a  
461 (10d) shows the daily averaged CATS extinction profiles in a black line, and 00, 06, 12 and 18  
462 UTC averaged in blue, green, yellow and red lines respectively, for the DJFMAM (JJASON)  
463 season. CATS extinction profiles for the daily average as well averages for the four selected

464 times are similar, suggesting that minor temporal variations in CATS extinctions can be expected  
465 for global averages.

466 Those global averages are dominated by CATS profiles from global oceans (Figure 10b  
467 and 10e), which also have small diurnal variations, as ~70% of the globe is covered by water. In  
468 comparison, noticeable diurnal changes in aerosol vertical distributions are found over land as  
469 shown in Figure 10c and 10f. For the DJFMAM season, at the 1 km altitude, the minimum and  
470 maximum aerosol extinctions are at 12 and 18 UTC respectively. Similarly, the minimum and  
471 maximum aerosol extinctions are at 18 and 6 UTC at the altitude of 400 m. For the JJASON  
472 season, the minimum aerosol extinction values are found at 12 UTC for the whole 0-2 km  
473 column, while the maximum aerosol extinction values are at 18UTC for 1.5 km and 0UTC for  
474 the 300-400 m altitude. Still, it should be noted that aerosol concentrations may be a function of  
475 local time, yet for a given UTC time, local times will vary by region. Also, due to solar  
476 contamination, nighttime retrievals from CATS are significantly and demonstrably less noisy than  
477 daytime retrievals, and this difference in sensor sensitivity between day and night may further  
478 affect the derived diurnal variations in CATS AOD and aerosol vertical profiles as shown in  
479 Figure 3 for individual retrievals. Still, no apparent solar pattern is detectable from Figure 8,  
480 and only minor diurnal variations are found for Figure 10a and 10d, which indicate that such a  
481 solar contamination may introduce noise but not bias to daytime aerosol retrievals, from a global  
482 mean perspective.

483 If we examine the mean global CATS extinction vertical profiles with respect to local  
484 time as shown in Figure 11, however, some distinct features appear. For example, Figure 11a  
485 and 11d suggests that on global average, the minimum and maximum aerosol extinction below 1  
486 km is found for 6:00 pm and 12:00 pm local time, respectively for both JJASON and DJFMAM

**Formatted:** Font: Not Italic

**Deleted:** nighttime retrievals from CATS are considered to be less noisy than daytime retrievals

489 seasons. Similar patterns are also observed for over global oceans. However, for over land  
490 cases, for both seasons, peak in aerosol extinction is found at the 500-1000 m layer for local  
491 noon, which is ~20-30% higher than daily mean values. This may indicate stronger solar heating  
492 at the surface and hence stronger near surface convection at local noon that brings near surface  
493 aerosol particles to a higher altitude.

494

### 495 **3.2.3 Diurnal variations of Aerosol Extinction on a Regional Scale (at local time)**

496 In this section, the diurnal variations of aerosol vertical distributions are studied as a  
497 function of local solar time for selected regions with high mean AODs as highlighted in Figure 6.  
498 We picked local solar time here as for those regional analyses, near 1 to 1 transformation can be  
499 achieved between UTC and local solar time. Also, as learned from the previous section, aerosol  
500 features are likely to have a local time dependency. A total of four regions, including Africa-  
501 north, Middle East, India and Northeast China, which show significant season all mean AODs in  
502 Figure 6, are selected for the DJFMAM season (Figure 12). For the JJASON season (Figure 13),  
503 in addition to the above mentioned 4 regions, the Africa-south region is also included due to  
504 biomass burning in the region during the Northern Hemisphere summer time. The  
505 Latitude/Longitude boundary of each selected region is described in Table 1. Regional-based  
506 analyses are also conducted for 4 (5) selected regions for the DJFMAM (JJASON) season at four  
507 local times: 0:00 am, 6:00 am, 12:00 pm and 6:00 pm, using quality assured CATS profiles.  
508 Generally, the maximum diurnal change in aerosol extinction is found at the altitude of below 1  
509 km for all regions as well for both seasons. Also, larger diurnal variations in vertical  
510 distributions of aerosol extinction are found for the JJASON season, in-comparing with the  
511 DJFMAM season, while regional-based differences are apparent.

512 For the Africa-north region, dominant aerosol types are dust and smoke aerosol for the  
513 DJFMAM season, and is dust for the JJASON season (e.g. Remer et al., 2008). Interestingly, the  
514 maximum aerosol extinction below 500m is found at 6:00 am for the DJFMAM season. While  
515 for the JJASON season, the maximum aerosol extinctions are found at 6:00 am for the whole 0-2  
516 km column, with a significant ~20% higher aerosol extinction from either daily mean or vertical  
517 profiles from 0:00 am, 12:00 pm and 6:00 pm. Note that 6:00 am in the Africa-north region  
518 corresponds to early morning, which has been identified in several studies (Fiedler et al., 2013;  
519 Ryder et al. 2015) as the time of day when nocturnal low-level jet breakdown causes large  
520 amounts of dust emission in this region. Thus, we suspect that this large 6:00 am peak in  
521 maximum aerosol extinctions may be the signal resulting from the low-level jet ejection  
522 mechanism captured on a regional scale. As the day progresses into the afternoon and early  
523 evening, we find the aerosol heights shifting upwards, likely related to the boundary layer's  
524 mixed layer development.

525 For the Middle East region, for the JJASON season, a daily maximum in aerosol  
526 extinction of  $\sim 0.13 \text{ km}^{-1}$  is found at local morning or early morning (0:00 am and 6:00 am), with  
527 a daily minimum of  $\sim 0.09 \text{ km}^{-1}$  found at local noon (12:00 pm), for the peak aerosol extinction  
528 layer that has a daily mean aerosol extinction of  $\sim 0.11 \text{ km}^{-1}$ . This translates to a  $\sim \pm 20\%$  daily  
529 variation for aerosol extinction for the peak aerosol extinction layer. Much smaller daily  
530 variation in aerosol extinction, however, is found for the same region for the DJFMAM season.

531 For the India region, for the JJASON season, a large peak in aerosol extinction of up to  
532 20% higher than daily mean is found at 6:00 am below 1 km. The minimum aerosol extinction is  
533 found at 0:00 am for the layer of  $\sim 400\text{-}1000 \text{ m}$ , and is overall  $\sim 10\%$  lower than the daily means.  
534 The minimum aerosol extinction is found at 6:00 pm for the layer below 400 m. For the

535 DJFMAM season, minimum aerosol extinctions are found at 12:00 pm for near the whole 0-2 km  
536 column, while for the layer below 500 m, the maximum aerosol extinction values are found at  
537 early morning (0:00 am and 6:00 am). This is consistent with the diurnal formation of  
538 significant haze.

539 For the Northeast China region, less diurnal variation is found for the DJFMAM season.  
540 Yet, a significant peak found at 1km for local noon (12:00 pm) for the JJASON season, which is  
541 ~30% higher than daily averages for the JJASON season. The reason for this elevated peak at  
542 regional local noon, however, is not known, although it may relate to the peak in surface  
543 Particulate Matter concentrations. Lastly, for the Africa-south region, biomass burning aerosols  
544 are prevalent during the summer time and thus only the JJASON season is analyzed. As shown  
545 in 13b, below 500m in altitude, lower extinction values are found for local afternoon (12:00 pm  
546 and 6:00 pm) and higher extinction values are found for local morning or early morning (0:00  
547 and 6:00 am). Still, the diurnal variation in aerosol vertical distribution is rather marginally for  
548 the region.

549

#### 550 **4.0 Conclusions**

551 Using CALIOP, MODIS and AERONET data, we evaluated CATS derived AODs as  
552 well as vertical distributions of aerosol extinctions for the study period of for Feb. 2015 – Oct.  
553 2017. CATS data (at 1064 nm) are further used to study variations in AODs and aerosol vertical  
554 distributions diurnally. We found:

555 (1) Quality assurance steps are critical for applying CATS data in aerosol related  
556 applications. With a 10% data loss due to QA steps, an improvement in correlation  
557 from 0.17 to 0.64 is found for the collocated CATS and AERONET AOD

558 comparisons. Using quality assured CATS data, reasonable agreements are found  
559 between CATS derived AODs and AODs from CALIOP, Aqua MODIS DT and  
560 Terra MODIS DT at the same local times, with correlations of 0.70, 0.75 and 0.71  
561 respectively.

562 (2) While the averaged vertical distributions from CATS compare reasonably well with  
563 that from CALIOP, differences in peak extinction altitudes are present. This may due  
564 to contamination of daytime aerosol detections over ocean by marine boundary layer  
565 clouds in the CATS V2-01 data products, which will hopefully be resolved in the  
566 future CATS V3-00 data.

567 (3) From the global mean perspective, minor changes are found for AODs at four  
568 selected times, namely 00, 06, 12 and 18 UTC. Yet noticeable diurnal variations in  
569 AODs of above 0.15 (at 1064 nm) are found for regions with extensive aerosol  
570 events, such as over North Africa, and India for the DJFMAM season, and over North  
571 and South of Africa, India and Middle East for the JJASON season.

572 (4) From the global mean perspective, changes are less noticeable for the averaged  
573 aerosol extinction profiles at 00, 06, 12 and 18 UTC. Yet, if the study is repeated  
574 with respect to local time, a peak in aerosol extinction is found for local noon and the  
575 minimum value in aerosol extinction is found at 6:00 pm local time for both JJASON  
576 and DJFMAM seasons. In particular, for over land cases, in both seasons, a lifted  
577 aerosol plume at 500-1000 m altitude (with the peak aerosol extinction that is ~20-  
578 30% higher than daily averages) is found at local noon, which may indicate the impact  
579 of strong surface solar heating as well as stronger near surface convection on aerosol  
580 vertical distributions.

581 (5) Larger diurnal variations are found at regions with heavy aerosol plumes such as  
582 North and South (summer season only) of Africa, Middle East, India and Eastern  
583 China. In particular, aerosol extinctions from 6:00 am over North Africa are ~20%  
584 higher than daily means as well other three times for the 0-2 km column for the  
585 JJASON season. We suspect this may be related to increase in dust concentrations  
586 due to breakdown of low level jets at early morning time for the region.

587 (6) Still, readers shall be aware that AOD retrievals at the 1064 nm are less sensitive to  
588 fine mode aerosols such as smoke and pollutant aerosols, compared to coarse mode  
589 aerosols such as dust aerosols. Thus, an investigation of diurnal variations of aerosol  
590 properties at the visible channel may be also needed for a future study.

591 This paper suggests that strong regional diurnal variations exist for both AOD and  
592 aerosol extinction profiles. Still, at present these conclusions are tentative, and will remain so  
593 until a comprehensive analysis of the CATS calibration accuracy and stability is completed.  
594 These results demonstrate the need for global aerosol measurements throughout the entire diurnal  
595 cycle to improve visibility and particulate matter forecasts as well as studies focused on aerosol  
596 climate applications.

Deleted: .

597  
598 **Author Contribution:**

599 Authors J. Zhang, J. S. Reid and L. Lee designed the study. L. lee worked on data processing for  
600 the project. J. E. Yorks guided L. lee on data processing. The manuscript was written with  
601 inputs from all coauthors.

602 **Acknowledgments:**

604 We acknowledge the support of ONR grant (N00014-16-1-2040) and NASA grant  
605 (NNX17AG52G) for this study. L. Lee is also partially supported by the NASA NESSF  
606 fellowship grant (NNX16A066H). J. S Reid's participation was supported by the Office of Naval  
607 Research Code 322 and 33. We thank the NASA AERONET team for the AERONET data used  
608 in this study.  
609

610 **References:**

611 Aerosol Product Application Team of the AWG Aerosols/Air Quality/Atmospheric  
612 Chemistry Team: GOES-R Advanced Baseline Imager (ABI) algorithm theoretical basis  
613 document for suspended matter/aerosol optical depth and aerosol size parameter,  
614 NOAA/NESDIS/STAR July 2012,  
615 <https://www.star.nesdis.noaa.gov/goesr/docs/ATBD/AOD.pdf> (last accessed on Nov. 17,  
616 2018).

617 Alfaro-Contreras, R., Zhang, J., Campbell, J. R., and Reid, J. S.: Investigating the frequency  
618 and trends in global above-cloud aerosol characteristics with CALIOP and OMI, *Atmos.*  
619 *Chem. Phys.*, 16, 47-69, doi:10.5194/acp-16-47-2016, 2016.

620 Campbell, J. R., Tackett, J. L., Reid, J. S., Zhang, J., Curtis, C. A., Hyer, E. J., Sessions, W.  
621 R., Westphal, D. L., Prospero, J. M., Welton, E. J., Omar, A. H., Vaughan, M. A., and  
622 Winker, D. M.: Evaluating nighttime CALIOP 0.532  $\mu\text{m}$  aerosol optical depth and  
623 extinction coefficient retrievals, *Atmos. Meas. Tech.*, 5, 2143-2160,  
624 <https://doi.org/10.5194/amt-5-2143-2012>, 2012.

625 CATS Algorithm Theoretical Basis Document:  
626 [https://cats.gsfc.nasa.gov/media/docs/CATS\\_ATBD\\_V1-02.pdf](https://cats.gsfc.nasa.gov/media/docs/CATS_ATBD_V1-02.pdf), 2016; accessed on  
627 [March 28, 2019.](#)

628 Christopher, S. A. and Zhang, J.: Daytime variation of shortwave direct radiative forcing of  
629 biomass burning aerosols from GOES 8 imager, *J. Atmos. Sci.*, 59, 681–691, 2002.

630 Eck, T. F., Holben, B. N., Reid, J. S., Mukelabai, M. M., Piketh, S. J., Torres, O., Jethva, H.  
631 T., Hyer, E. J., Ward, D. E., Dubovik, O., and Sinyuk, A.: A seasonal trend of single  
632 scattering albedo in southern African biomass-burning particles: Implications for satellite

633 products and estimates of emissions for the world's largest biomass-burning source, J.  
634 Geophys. Res.-Atmos., 118, 6414–6432, 2013.

635 Fiedler, S., Schepanski, K., Heinold, B., Knippertz, P., and Tegen, I.: Climatology of  
636 nocturnal low-level jets over North Africa and implications for modeling mineral dust  
637 emission, J. Geophys. Res. Atmos., 118, 6100–6121, doi: 10.1002/jgrd.50394, 2013.

638 Giglio, L., Kendall, J.D., Mack, R.: A multi-year active fire dataset for the tropics derived  
639 from the TRMM VIRS,. International Journal of Remote Sensing 24, 4505-4525, 2003.

640 Giles, D. M., Sinyuk, A., Sorokin, M. S., Schafer, J. S., Smirnov, A., Slutsker, I., Eck, T. F.,  
641 Holben, B. N., Lewis, J., Campbell, J., Welton, E. J., Korkin, S., and Lyapustin, A.:  
642 Advancements in the Aerosol Robotic Network (AERONET) Version 3 Database –  
643 Automated Near Real-Time Quality Control Algorithm with Improved Cloud Screening  
644 for Sun Photometer Aerosol Optical Depth (AOD) Measurements, Atmos. Meas. Tech.  
645 Discuss., <https://doi.org/10.5194/amt-2018-272>, in review, 2018.

646 Heinold, B., Knippertz, P., Marsham, J. H., Fiedler, S., Dixon, N. S., Schepanski, K.,  
647 Laurent, B., and Tegen, I.: The role of deep convection and nocturnal low-level jets for  
648 dust emission in summertime West Africa: Estimates from convection-permitting  
649 simulations, J. Geophys. Res. Atmos., 118, 4385–4400, doi:10.1002/jgrd.50402, 2013.

650 Holben, B. N., and coauthors: AERONET—A Federated Instrument Network and Data  
651 Archive for Aerosol Characterization. Remote Sensing of Environment, 66(1), 1–16.  
652 [https://doi.org/10.1016/S0034-4257\(98\)00031-5](https://doi.org/10.1016/S0034-4257(98)00031-5), 1998.

653 Hyer, E. J., Reid, J. S., Prins, E. M., Hoffman, J. P., Schmidt, C. C., Miettinen, J. I., and  
654 Giglio, L.: Different views of fire activity over Indonesia and Malaysia from polar and  
655 geostationary satellite observations, *Atmos. Res.*, 122, 504-519, 2013.

656 Kaku K. C., Reid, J. S., Hand, J. L., Edgerton, E. S., Holben, B. N., Zhang, J., and Holz, R.  
657 E.: Assessing the challenges of surface-level aerosol mass estimates from remote sensing  
658 during the SEAC4RS campaign: Baseline surface observations and remote sensing in the  
659 Southeastern United States, *JGR*, doi: 10.1029/2017JD028074, 2018.

660 Levy, R. C., Mattoo, S., Munchak, L. A., Remer, L. A., Sayer, A. M., Patadia, F., and Hsu,  
661 N. C.: The Collection 6 MODIS aerosol products over land and ocean. *Atmos. Meas.*  
662 *Tech.*, 6(11), 2989–3034. <https://doi.org/10.5194/amt-6-2989-2013>, 2013.

663 Liu, Z., and coauthors: The CALIPSO Lidar Cloud and Aerosol Discrimination: Version 2  
664 Algorithm and Initial Assessment of Performance, *J. Atmos. Oceanic Technol.*, 26, 1198–  
665 1213, 2009.

666 Lynch, P., Reid, J. S., Westphal, D. L., Zhang, J., Hogan, T. F., Hyer, E. J., Curtis, C. A.,  
667 Hegg, D. A., Shi, Y., Campbell, J. R., Rubin, J. I., Sessions, W. R., Turk, F. J., and  
668 Walker, A. L.: An 11-year global gridded aerosol optical thickness reanalysis (v1.0) for  
669 atmospheric and climate sciences, *Geosci. Model Dev.*, 9, 1489-1522,  
670 <https://doi.org/10.5194/gmd-9-1489-2016>, 2016.

671 Mbourou, G. N., Berand, J. J., and Nicholson, S. E.: The diurnal and seasonal cycle of wind-  
672 borne dust over Africa north of the equator, *J. Appl. Meteor.*, 36, 868-882, 1997.

673 McGill, M. J., Yorks, J. E., Scott, V. S., Kupchock, A. W., and Selmer, P. A.: The Cloud-  
674 Aerosol Transport System (CATS): A technology demonstration on the International  
675 Space Station, *Proc. SPIE 9612, Lidar Remote Sensing for Environmental Monitoring*  
676 *XV*, 96120A, doi:10.1117/12.2190841, 2015.

677 Noel, V., Chepfer, H., Chiriaco, M., and Yorks J. E.: The diurnal cycle of cloud profiles over  
678 land and ocean between 51° S and 51° N, seen by the CATS spaceborne lidar from the

679 International Space Station, Atmos. Chem. Phys., 18, 9457-9473,  
680 <https://doi.org/10.5194/acp-18-9457-2018>, 2018.

681 Omar, A. H., Winker, D. M., Tackett, J. L., Giles, D. M., Kar, J., Liu, Z., Vaughan, M. A.,  
682 Powell, K. A., and Trepte C. R.: CALIOP and AERONET aerosol optical depth  
683 comparisons: One size fits none, J. Geophys. Res. Atmos., 118, 4748–4766, doi:  
684 10.1002/jgrd.50330, 2013.

685 Rajapakshe, C., Zhang, Z., Yorks, J. E., Yu, H., Tan, Q., Meyer, K., Platnick, S.: Seasonally  
686 Transported Aerosol Layers over Southeast Atlantic are Closer to Underlying Clouds  
687 than Previously Reported, Geophys. Res. Lett., 44, doi:10.1002/2017GL073559, 2017.

688 Redemann, J., Vaughan, M. A., Zhang, Q., Shinozuka, Y., Russell, P. B., Livingston, J. M.,  
689 ... Remer, L. A.: The comparison of MODIS-Aqua (C5) and CALIOP (V2 & V3) aerosol  
690 optical depth. Atmospheric Chemistry and Physics, 12(6), 3025–3043.  
691 <https://doi.org/https://doi.org/10.5194/acp-12-3025-2012>, 2012.

692 Reid, J.S., Eck, T. F., Christopher, S. A., Hobbs, P. V., and Holben B. R.: Use of the  
693 Angstrom exponent to estimate the variability of optical and physical properties of aging  
694 smoke particles in Brazil, J. Geophys. Res., 104, 27,489-27,489, 1999.

695 Remer, L. A., and coauthors: Global aerosol climatology from the MODIS satellite sensors,  
696 J. Geophys. Res., 113, D14S07, doi: 10.1029/2007JD009661, 2008.

697 ~~Remer, L.A., Y.J. Kaufman, D. Tanré, S. Mattoo, D.A. Chu, J.V. Martins, R. Li, C. Ichoku,~~  
698 ~~R.C. Levy, R.G. Kleidman, T.F. Eck, E. Vermote, and B.N. Holben. The MODIS~~  
699 ~~Aerosol Algorithm, Products, and Validation, J. Atmos. Sci., 62, 947–973,~~  
700 ~~<https://doi.org/10.1175/JAS3385.1>, 2005.~~

Formatted: Justified, Indent: Left: 0.25", Hanging: 0.25",  
Line spacing: Double

Deleted: .

Formatted: Font: Not Italic, Not Highlight

702 Ryder, C. L., McQuaid, J. B., Flamant, C., Rosenberg, P. D., Washington, R., Brindley, H.  
703 E., Highwood, E. J., Marsham, J. H., Parker, D. J., Todd, M. C., Banks, J. R., Brooke, J.  
704 K., Engelstaedter, S., Estelles, V., Formenti, P., Garcia-Carreras, L., Kocha, C., Marengo,  
705 F., Sodemann, H., Allen, C. J. T., Bourdon, A., Bart, M., Cavazos-Guerra, C.,  
706 Chevaillier, S., Crosier, J., Darbyshire, E., Dean, A. R., Dorsey, J. R., Kent, J.,  
707 O'Sullivan, D., Schepanski, K., Szpek, K., Trembath, J., and Woolley, A.: Advances in  
708 understanding mineral dust and boundary layer processes over the Sahara from Fennec  
709 aircraft observations, *Atmos. Chem. Phys.*, 15, 8479-8520, [https://doi.org/10.5194/acp-](https://doi.org/10.5194/acp-15-8479-2015)  
710 15-8479-2015, 2015.

711 Shi Y., Zhang, J., Reid, J. S., Hyer, E., and Hsu, N. C.: Critical evaluation of the MODIS  
712 Deep Blue aerosol optical depth product for data assimilation over North Africa, *Atmos.*  
713 *Meas. Tech.*, 6, 949-969, doi:10.5194/amt-6-949-2013, 2013.

714 Shi Y., Zhang J., Reid J. S., Hyer E. J., Eck T. F., and Holben B. N.: A critical examination  
715 of spatial biases between MODIS and MISR aerosol products – application for potential  
716 AERONET deployment, *Atmos. Meas. Tech.*, 4, 2823–2836, 2011.

717 Stephens, G. L., and coauthors: The CLOUDSAT mission and the A-TRAIN, *Bulletin of the*  
718 *American Meteorological Society*, 83(12), 1771–1790. [https://doi.org/10.1175/BAMS-](https://doi.org/10.1175/BAMS-83-12-1771)  
719 [83-12-1771](https://doi.org/10.1175/BAMS-83-12-1771), 2002.

720 Tiwari, S., Srivastava, A. K., Bisht, D. S., Parmita, P., Srivastava, M. K., and Atri, S. D.:  
721 Diurnal and seasonal variation of black carbon and PM<sub>2.5</sub> over New Delhi, India:  
722 Influence of meteorology, *Atmos. Res.*, 125, 50-62, doi:10.1016/j.atmos.res.2013.01.011,  
723 2013.

724 Toth, T. D., Campbell, J. R., Reid, J. S., Tackett, J. L., Vaughan, M. A., Zhang, J., &  
725 Marquis, J. W.: Minimum aerosol layer detection sensitivities and their subsequent  
726 impacts on aerosol optical thickness retrievals in CALIPSO level 2 data products.  
727 Atmospheric Measurement Techniques, 11(1), 499–514.  
728 <https://doi.org/https://doi.org/10.5194/amt-11-499-2018>, 2018.

729 Toth, T. D., Zhang, J., Campbell, J. R., Reid, J. S., & Vaughan, M. A.: Temporal variability  
730 of aerosol optical thickness vertical distribution observed from CALIOP, Journal of  
731 Geophysical Research: Atmospheres, 121(15), 9117–9139.  
732 <https://doi.org/10.1002/2015JD024668>, 2016.

733 Vaughan, M., Garnier, A., Josset, D., Avery, M., Lee, K.-P., Liu, Z., Hunt, W., Pelon, J.,  
734 Tackett, J., Getzewich, B., Kar, J., and Burton, S.: CALIPSO Lidar Calibration at 1064  
735 nm: Version 4 Algorithm, in preparation, 2018.

736 Wang, J., Liu, X., Christopher, S. A., Reid, J. S., Reid, E. A., and Maring, H.: The effects of  
737 non-sphericity on geostationary satellite retrievals of dust aerosols, Geophys. Res. Lett.,  
738 30(24), 2293, doi:10.1029/2003GL018697, 2003.

739 Winker, D. M., and coauthors: Overview of the CALIPSO Mission and CALIOP Data  
740 Processing Algorithms. Journal of Atmospheric and Oceanic Technology, 26(11), 2310–  
741 2323. <https://doi.org/10.1175/2009JTECHA1281.1>, 2009.

742 Yorks, J. E., McGill, M. J., Palm, S. P., Hlavka, D. L., Selmer, P. A., Nowottnick, E.,  
743 Vaughan, M. A., Rodier, S., and Hart W. D.: An Overview of the CATS Level 1 Data  
744 Products and Processing Algorithms, Geophys. Res. Lett., 43,  
745 doi:[10.1002/2016GL068006](https://doi.org/10.1002/2016GL068006), 2016.

**Deleted:** Yorks, J. E., Palm, S. P., Hlavka, D. L., McGill, M. J., Nowottnick, E., Selmer, P. A., Hart, W. D.: The Cloud-Aerosol Transport System (CATS)<sup>¶</sup> algorithm theoretical basis document. Available at [http://cats.gsfc.nasa.gov/media/docs/CATS\\_ATBD.pdf](http://cats.gsfc.nasa.gov/media/docs/CATS_ATBD.pdf), 2015.<sup>¶</sup>

751       Yorks, J. E., Rodier, S.D., Nowottnick, E., Selmer, P.A., McGill, M.J., Palm, S.P., and  
752           Vaughan, M. A.: CATS Level 2 Vertical Feature Mask Algorithms and Data Products:  
753           An Overview and Initial Assessment, Atmos. Meas. Tech. Discuss., in preparation.

754       Yoshida M., Kikuchi, M., Nagao, T. M., Murakami, H., Nomaki, T., and Higurashi, A.:  
755           Common Retrieval of Aerosol Properties for Imaging Satellite Sensors, Journal of the  
756           Meteorological Society of Japan. Ser. II, Article ID 2018-039, [Advance publication],  
757           <https://doi.org/10.2151/jmsj.2018-039>, 2018.

758       Zhao, X. J., Zhang, X. L., Xu, X. F., Xu, J., Meng, W., and Pu, WW.: Seasonal and diurnal  
759           variation of ambient PM<sub>2.5</sub> concentrations in urban and rural environments in Beijing,  
760           Atmos. Environ., 43, 2893-2900, doi: 10.106/j.atmosenv.2009.03.009., 2009.

761

762 Table 1. Geographic ranges, height above ground level of maximum extinction, diurnal  
 763 extinction range at height of maximum extinction, and time (local) of peak extinction for the  
 764 boxed red regions in Figure 6 and vertical profiles shown in Figures 12 and 13.

DJFMAM/JJASON					
Region	Latitude	Longitude	Height AGL (m) of Max. Extinction	Extinction Range ( $\text{km}^{-1}$ ) at Height AGL of Max. Extinction	Time of Peak Extinction at Height AGL of Max. Extinction
India	7.5°N - 32.5°N	65°E - 85°E	180/240	0.109-0.131/0.138-0.182	6 am/6 am
Africa - North	2.5°N - 22.5°N	35°W - 20°E	420/480	0.107-0.130/0.098-0.121	12 pm/6 am
Africa - South	17.5°S - 2.5°N	0° - 30°E	/420	/0.090-0.100	/6 am
Middle East	12.5°N - 27.5°N	35°E - 50°E	240/180	0.093-0.116/0.081-0.135	6 am/0 am
China	27.5°N - 37.5°N	110°E - 120°E	240/240	0.107-0.154/0.085-0.133	6 am/6 am

765

766

767

768 Table 2. CALIOP and CATS mean aerosol optical depth for regions as highlighted in Figure 6  
769 and globally between +/- 52° latitude.

Formatted: Font: 12 pt, Not Italic, Font color: Auto

Formatted: Caption, Keep with next

Formatted: Font: 12 pt, Not Italic, Font color: Auto

Formatted Table

Region	Latitude	Longitude	Mean CATS AOD (DJFMAM/JJASON)	Mean CALIOP AOD (DJFMAM/JJASON)
Global	52°S-52°N	180°W-180°E	0.09/0.10	0.09/0.09
India	7.5°N - 32.5°N	65°E - 85°E	0.22/0.26	0.22 /0.28
Africa - North	2.5°N - 22.5°N	35°W - 20°E	0.26/0.23	0.30 /0.25
Africa - South	17.5°S - 2.5°N	0° - 30°E	0.14/0.22	0.15 /0.13
Middle East	12.5°N - 27.5°N	35°E - 50°E	0.22/0.33	0.26/0.35
China	27.5°N - 37.5°N	110°E - 120°E	0.19/0.18	0.21 /0.16

770

Formatted: Line spacing: Multiple 1.08 li

771 **Figure Captions**

772  
773 **Figure 1.** Collocated AERONET 1020 nm AOT vs. CATS 1064 nm AOD a) without CATS QA  
774 applied, and b) with CATS QA applied.

775 **Figure 2.** Collocated MODIS C6.1 a) Terra and b) Aqua estimated 1064 nm AOD vs. CATS  
776 1064 nm AOD with CATS QA applied.

777 **Figure 3.** Collocated CALIOP 1064 nm AOD vs. CATS 1064 nm AOD with CATS QA applied  
778 for a) both day and night, b) nighttime over-land, c) nighttime over-water, d) daytime over-land,  
779 e) daytime over-water.

780 **Figure 4:** CATS 1064 nm AOD a) as a function of local time for the globe, and b) as a function  
781 of local time for areas south of -25 degrees. The difference between CATS 1064 nm AOD and  
782 AERONET 1020 nm AOD as a function of local time is shown in c). The mean is represented  
783 by the blue line, while the median is the green line.

784 **Figure 5.** CATS and CALIOP vertical profiles of 1064 nm extinction for a) all profiles, b)  
785 daytime only, c) nighttime only, d) over-water, and e) over land.

786 **Figure 6.** Mean AOD (1064 nm) by season for a) DJFMAM CATS, b) JJASON CATS, c)  
787 DJFMAM CALIOP, d) JJASON CALIOP, e) DJFMAM MODIS Aqua, and f) JJASON MODIS  
788 Aqua. Red boxes indicate locations of regional vertical distributions in Figures 12 and 13.

789 **Figure 7.** Mean CATS AOD (1064 nm) by season for a) DJFMAM below 1 km AGL, b)  
790 JJASON below 1 km AGL, c) DJFMAM 1-2 km AGL, d) JJASON 1-2 km AGL, e) DJFMAM  
791 above 2 km AGL, and f) JJASON above 2 km AGL.

792 **Figure 8.** Seasonal Mean AOD (1064 nm) binned by every 6-hours for a) DJFMAM 0 UTC, b)  
793 JJASON 0 UTC, c) DJFMAM 6 UTC, d) JJASON 6 UTC, e) DJFMAM 12 UTC, f) JJASON 12  
794 UTC, g) DJFMAM 18 UTC, and h) JJASON 18 UTC.

795 **Figure 9.** Maximum minus minimum mean seasonal AOD (1064 nm) for a) DJFMAM, and b)  
796 JJASON.

797 **Figure 10.** Global mean 6-hourly vertical profiles of CATS 1064 nm extinction for a) DJFMAM  
798 all profiles, b) DJFMAM water profiles, c) DJFMAM not-water profiles, e) JJASON all profiles,  
799 f) JJASON water profiles, g) JJASON not-water profiles.

800 **Figure 11.** Global mean 6-hourly local time (0:00 am, 6:00 am, 12:00 pm and 6:00 pm) vertical  
801 profiles of CATS 1064 nm extinction for a) DJFMAM all profiles, b) DJFMAM water profiles,  
802 c) DJFMAM not-water profiles, d) JJASON all profiles, e) JJASON water profiles, f) JJASON  
803 not-water profiles.

804 **Figure 12.** DJFMAM 6-hourly average (local time; 0:00 am, 6:00 am, 12:00 pm and 6:00 pm)  
805 vertical profiles of CATS 1064 nm for locations shown in Figure 6a; a) Africa-north, b) Middle  
806 East, c) India, and d) Northeast China.

807

808 **Figure 13.** JJASON 6-hourly average (local time; 0:00 am, 6:00 am, 12:00 pm and 6:00 pm)  
809 vertical profiles of CATS 1064 nm for locations shown in Figure 6b; a) Africa-north, b) Africa-  
810 south, c) Middle East, d) India, and e) Northeast China.  
811

**Deleted:** ¶  
**Figure 14.** Relative difference between CATS and CALIOP 1064 nm extinction as a function of height for all profiles.¶  
**Formatted:** Font: Not Bold

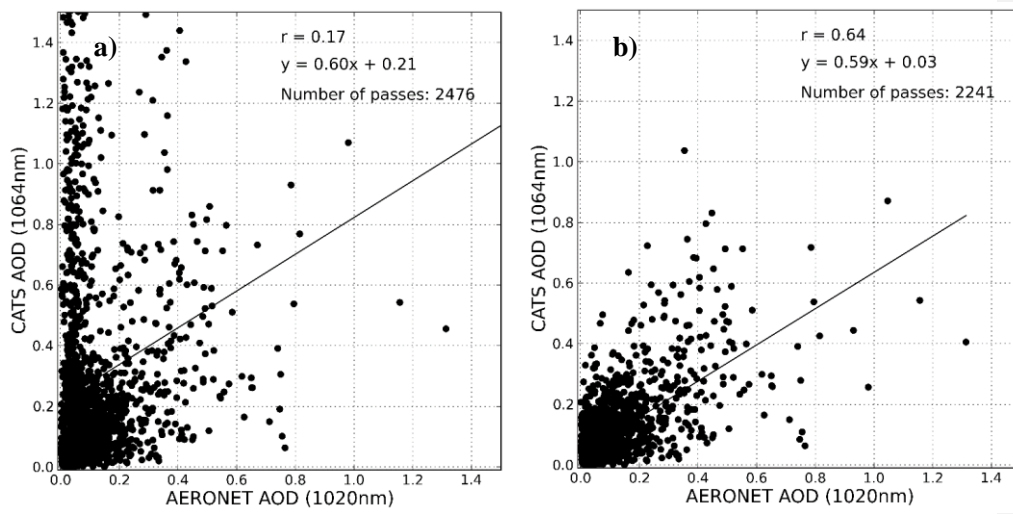


Figure 1. Collocated AERONET 1020 nm AOT vs. CATS 1064 nm AOD a) without CATS QA applied, and b) with CATS QA applied.

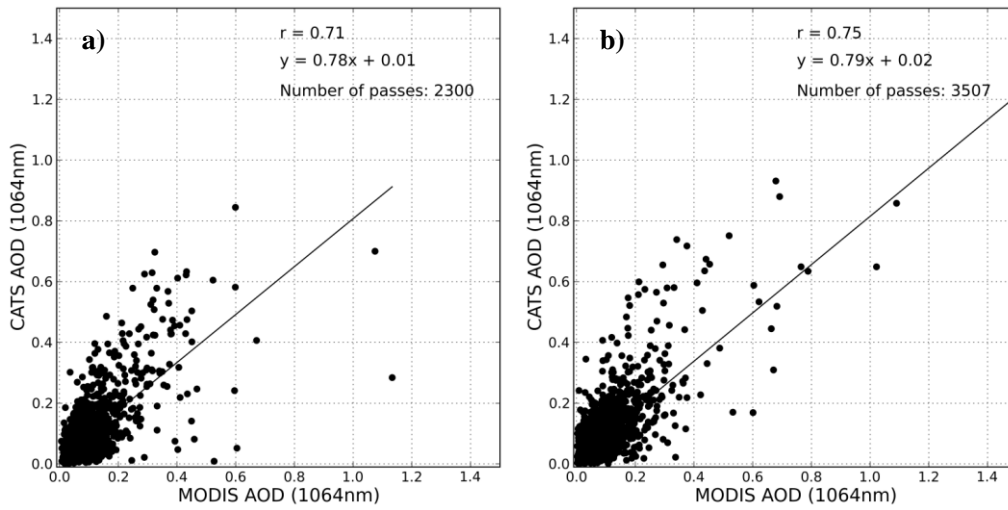


Figure 2. Collocated MODIS C6.1 a) Terra and b) Aqua estimated 1064 nm AOD vs. CATS 1064 nm AOD with CATS QA applied.

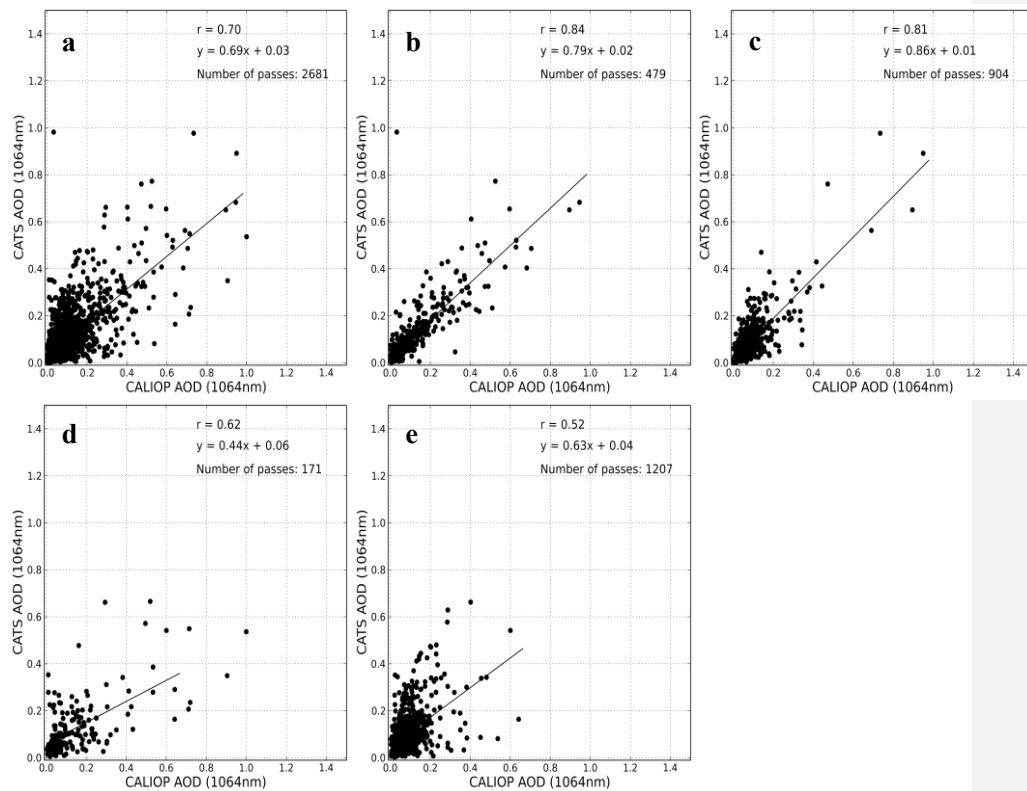


Figure 3. Collocated CALIOP 1064 nm AOD vs. CATS 1064 nm AOD with CATS QA applied for a) both day and night, b) nighttime over-land, c) nighttime over-water, d) daytime over-land, e) daytime over-water.

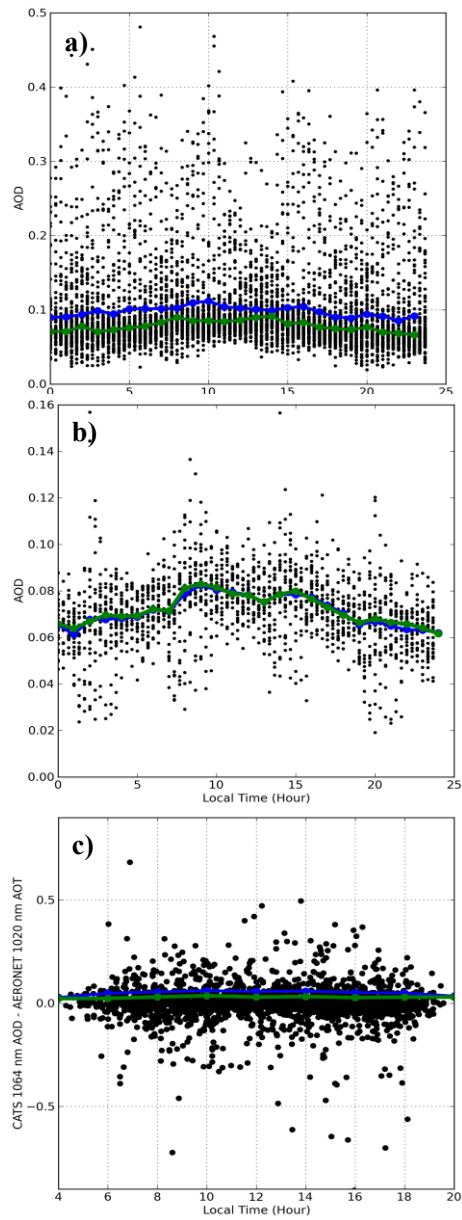


Figure 4. CATS 1064 nm AOD a) as a function of local time for the globe, and b) as a function of local time for areas south of  $-25$  degrees. The difference between CATS 1064 nm AOD and AERONET 1020 nm AOD as a function of local time is shown in c). The mean is represented by the blue line, while the median is the green line.

819  
820  
821  
822

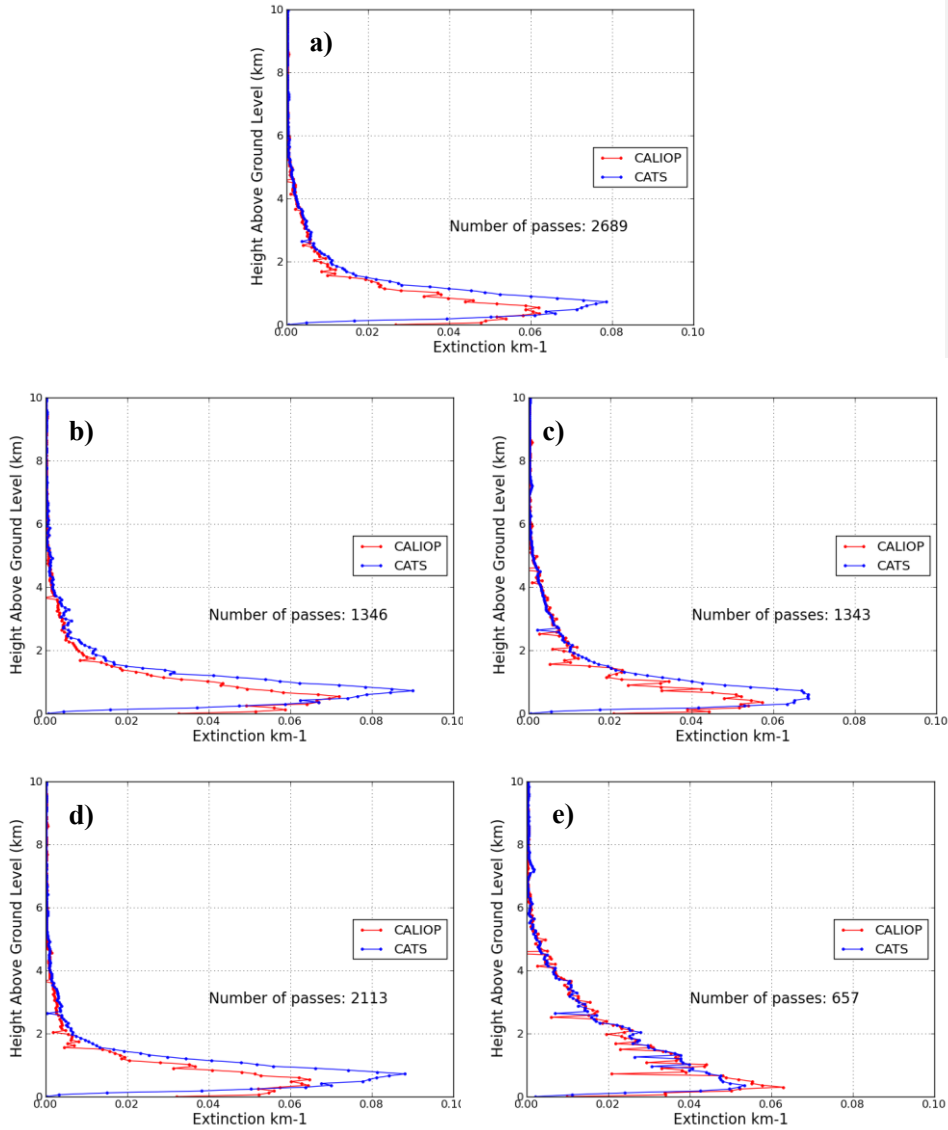


Figure 5. CATS and CALIOP vertical profiles of 1064 nm extinction for a) all profiles, b) daytime only, c) nighttime only, d) over-water, and e) over land.

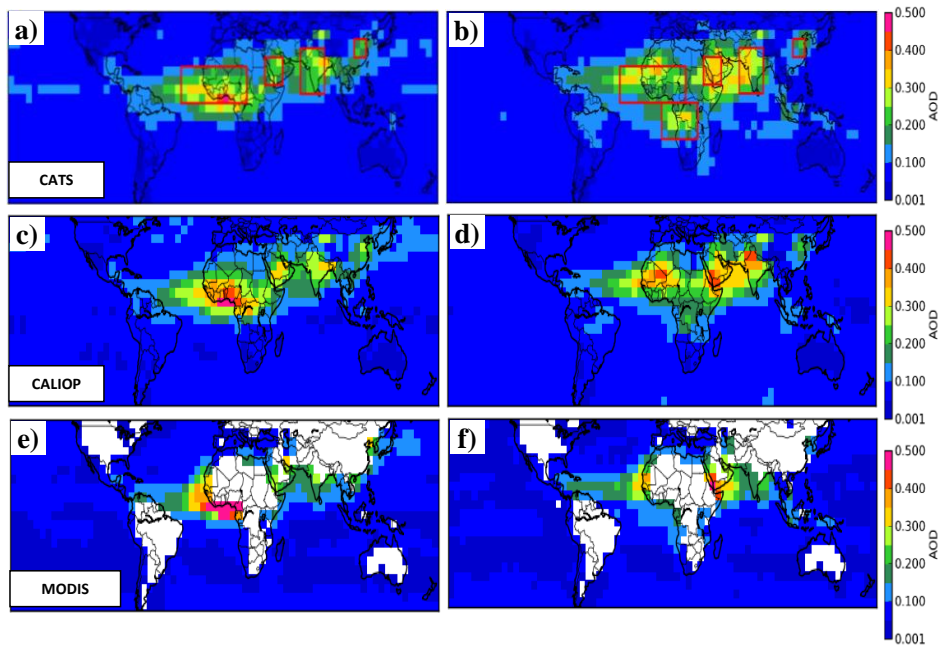


Figure 6. Mean AOD (1064 nm) by season for a) DJFMAM CATS, b) JJASON CATS, c) DJFMAM CALIOP, d) JJASON CALIOP, e) DJFMAM MODIS Aqua, and f) JJASON MODIS Aqua. Red boxes indicate locations of regional vertical distributions in Figures 12 and 13.

823  
 824  
 825  
 826  
 827  
 828  
 829

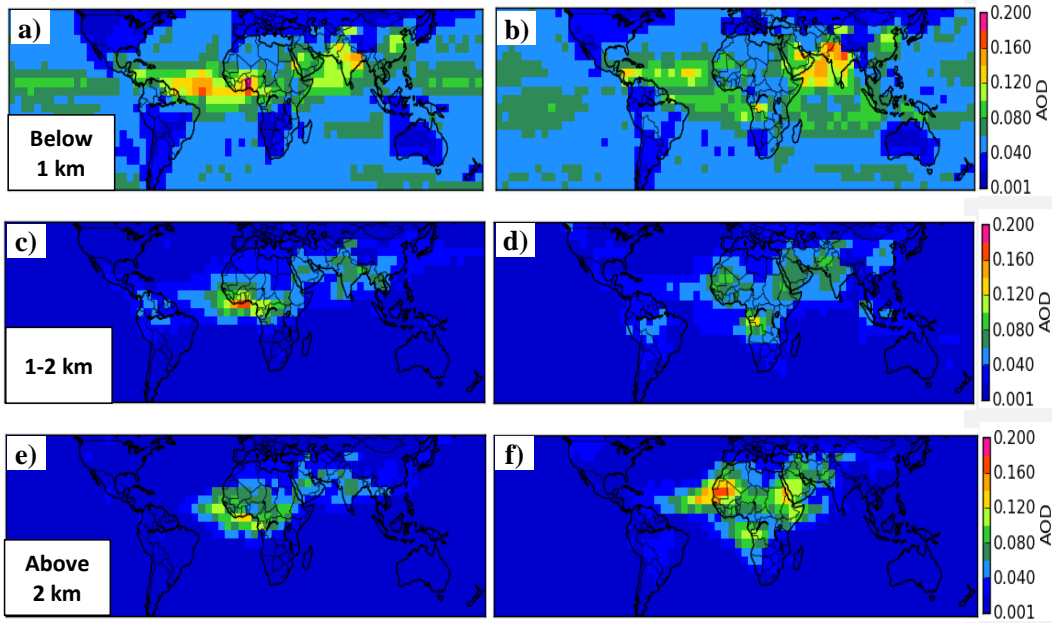


Figure 7. Mean CATS AOD (1064 nm) by season for a) DJFMAM below 1km AGL, b) JJASON below 1 km AGL, c) DJFMAM 1-2 km AGL, d) JJASON 1-2 km AGL, e) DJFMAM above 2 km AGL, and f) JJASON above 2 km AGL. Deleted: :

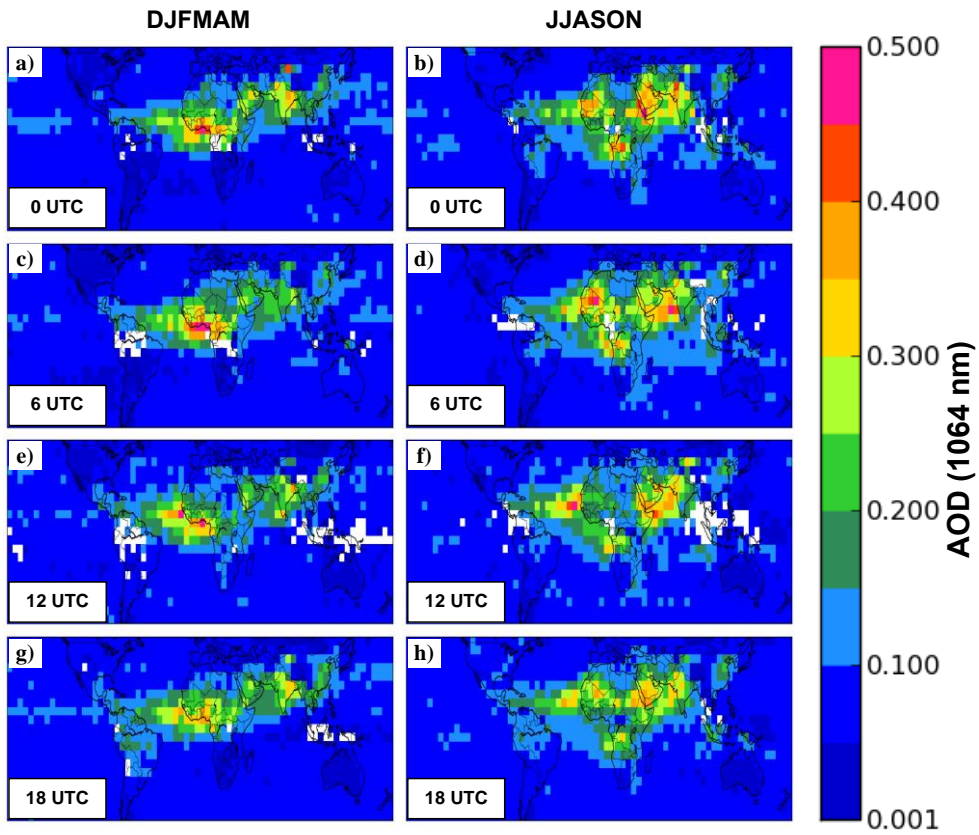


Figure 8. Seasonal Mean AOD (1064 nm) binned by every 6-hours for a) DJFMAM 0 UTC, b) JJASON 0 UTC, c) DJFMAM 6 UTC, d) JJASON 6 UTC, e) DJFMAM 12 UTC, f) JJASON 12 UTC, g) DJFMAM 18 UTC, and h) JJASON 18 UTC.

832

833

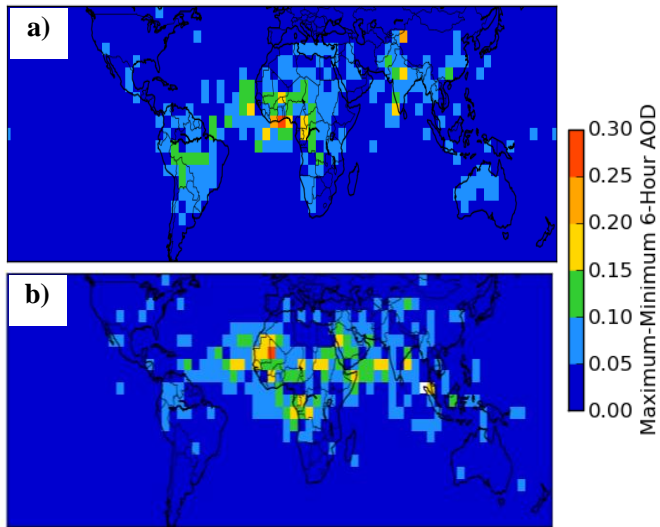
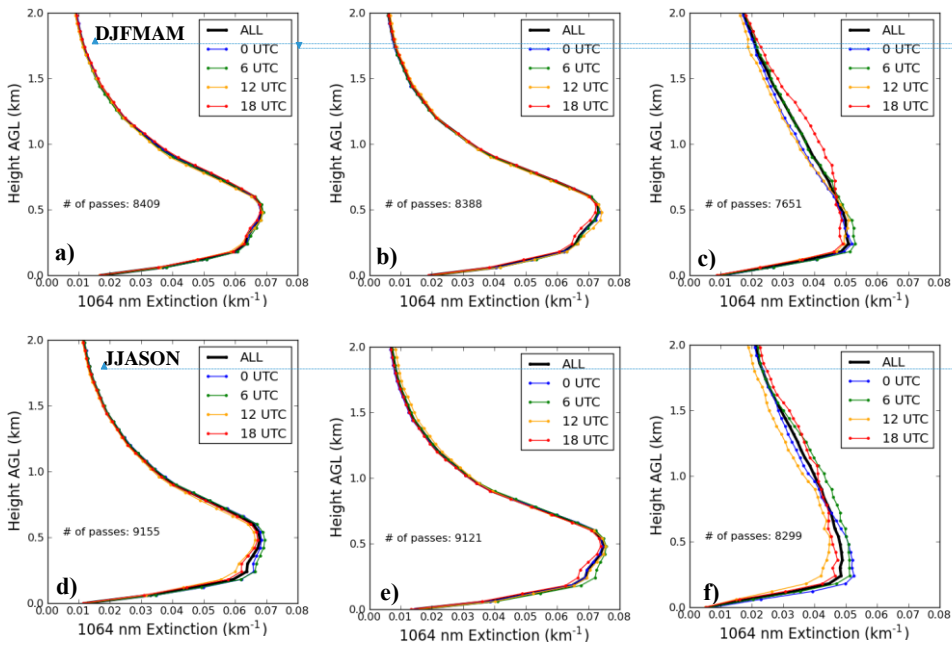


Figure 9. Maximum minus minimum mean seasonal AOD (1064 nm) for a) DJFMAM, and b) JJASON.

834  
835



Deleted: <object>  
Formatted: Font: 10 pt

Formatted: Font: 10 pt

Figure 10. Global mean 6-hourly vertical profiles of CATS 1064 nm extinction for a) DJFMAM all profiles, b) DJFMAM water profiles, c) DJFMAM not-water profiles, d) JJASON all profiles, e) JJASON water profiles, f) JJASON not-water profiles.

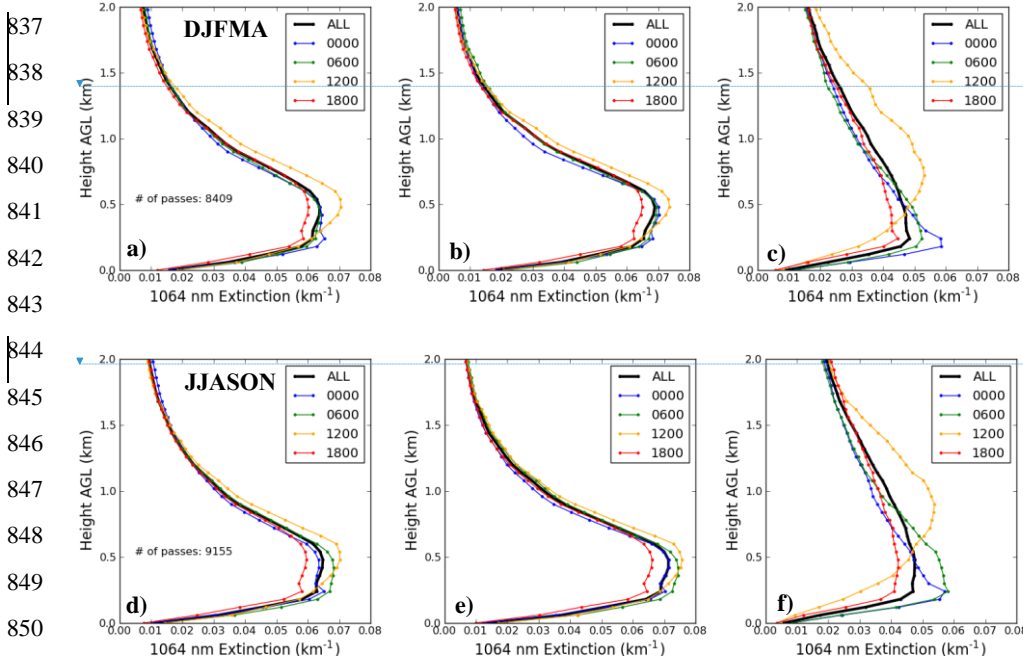


Figure 11. Global mean 6-hourly local time (0:00 am, 6:00 am, 12:00 pm and 6:00 pm) vertical profiles of CATS 1064 nm extinction for a) DJFMAM all profiles, b) DJFMAM water profiles, c) DJFMAM not-water profiles, d) JJASON all profiles, e) JJASON water profiles, f) JJASON not-water profiles.

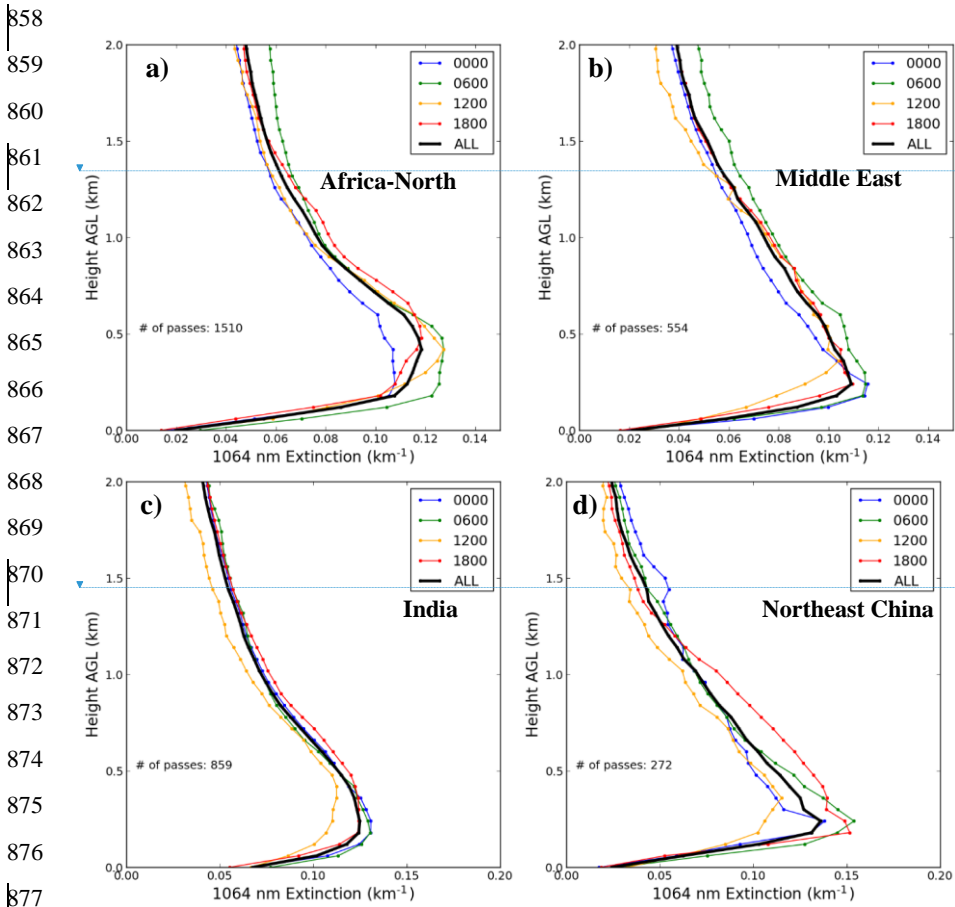


Figure 12. DJFMAM 6-hourly average (local time; 0:00 am, 6:00 am, 12:00 pm and 6:00 pm) vertical profiles of CATS 1064 nm for locations shown in Figure 6a; a) Africa-north, b) Middle East, c) India, and d) Northeast China.

Deleted: <object><object>

Deleted: <object><object>

Formatted: Font: 12 pt, Not Italic, Font color: Auto

Formatted: Caption

888  
889  
890  
891  
892  
893  
894  
895  
896  
897  
898  
899  
900  
901

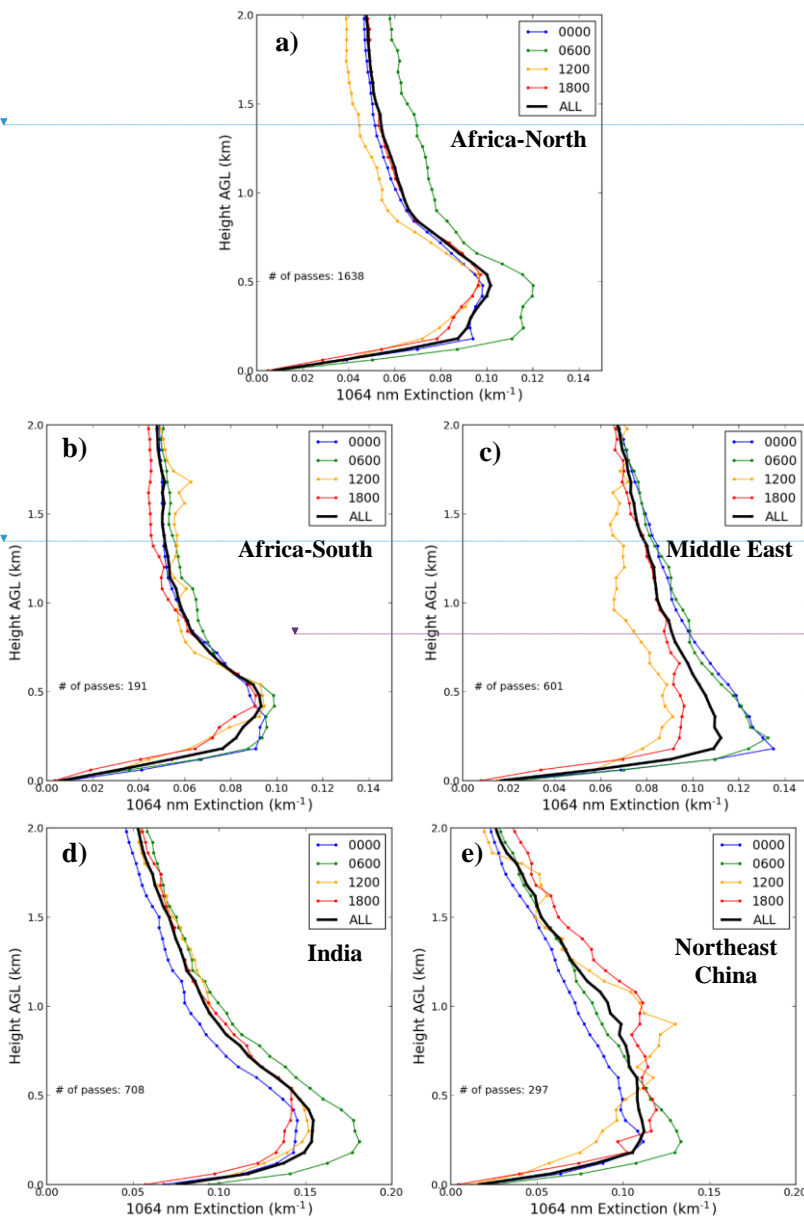
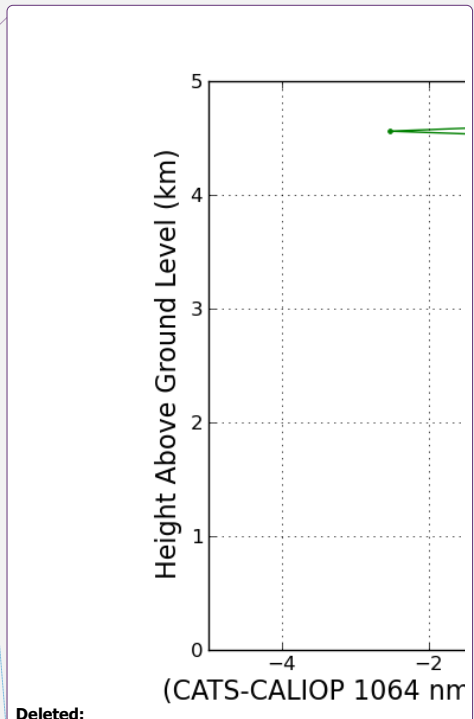


Figure 13. JJASON 6-hourly average (local time; 0:00 am, 6:00 am, 12:00 pm and 6:00 pm) vertical profiles of CATS 1064 nm for locations shown in Figure 6b; a) Africa-north, b) Africa-south, c) Middle East, d) India, and e) Northeast China.

Deleted: <object>

Deleted: <object><object>

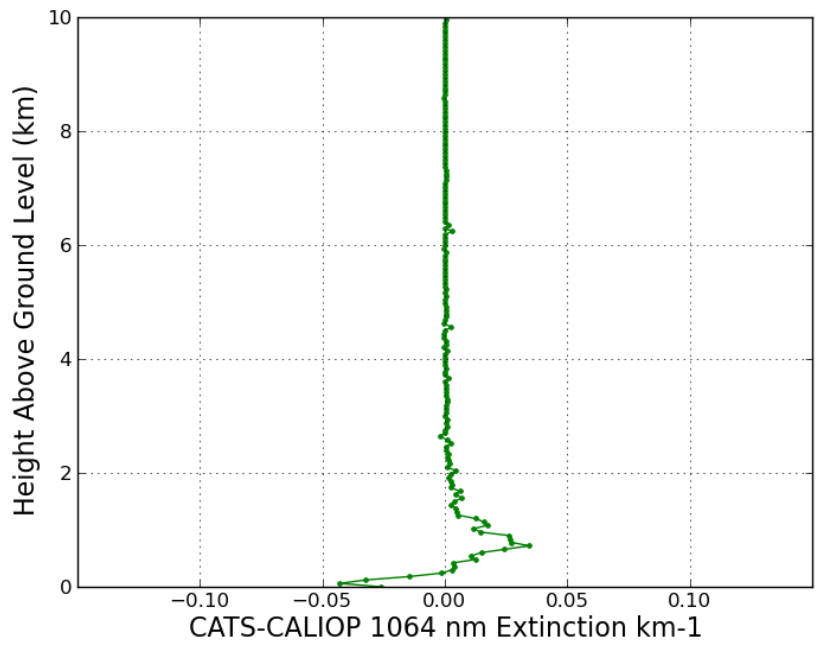


Deleted:  
Formatted: Keep with next

905 Appendix A

906 The difference between CATS and CALIOP mean 1064 nm extinction for all collocated profiles  
907 as shown in Figure 5a was plotted as a function of height.

**Deleted:** Figure 14. Relative difference between CATS and CALIOP 1064 nm extinction as a function of height for all profiles.



909 Figure A1. Difference between CATS and CALIOP mean 1064 nm extinction for all collocated profiles as a function of height.

**Formatted:** Font: 12 pt, Not Italic

**Formatted:** Caption

**Formatted:** Font: 12 pt, Not Italic

**Formatted:** Space After: 0 pt, Line spacing: single